# COMPUTERIZED TECHNIQUES

# COMPUTIZED TECHNIQUES

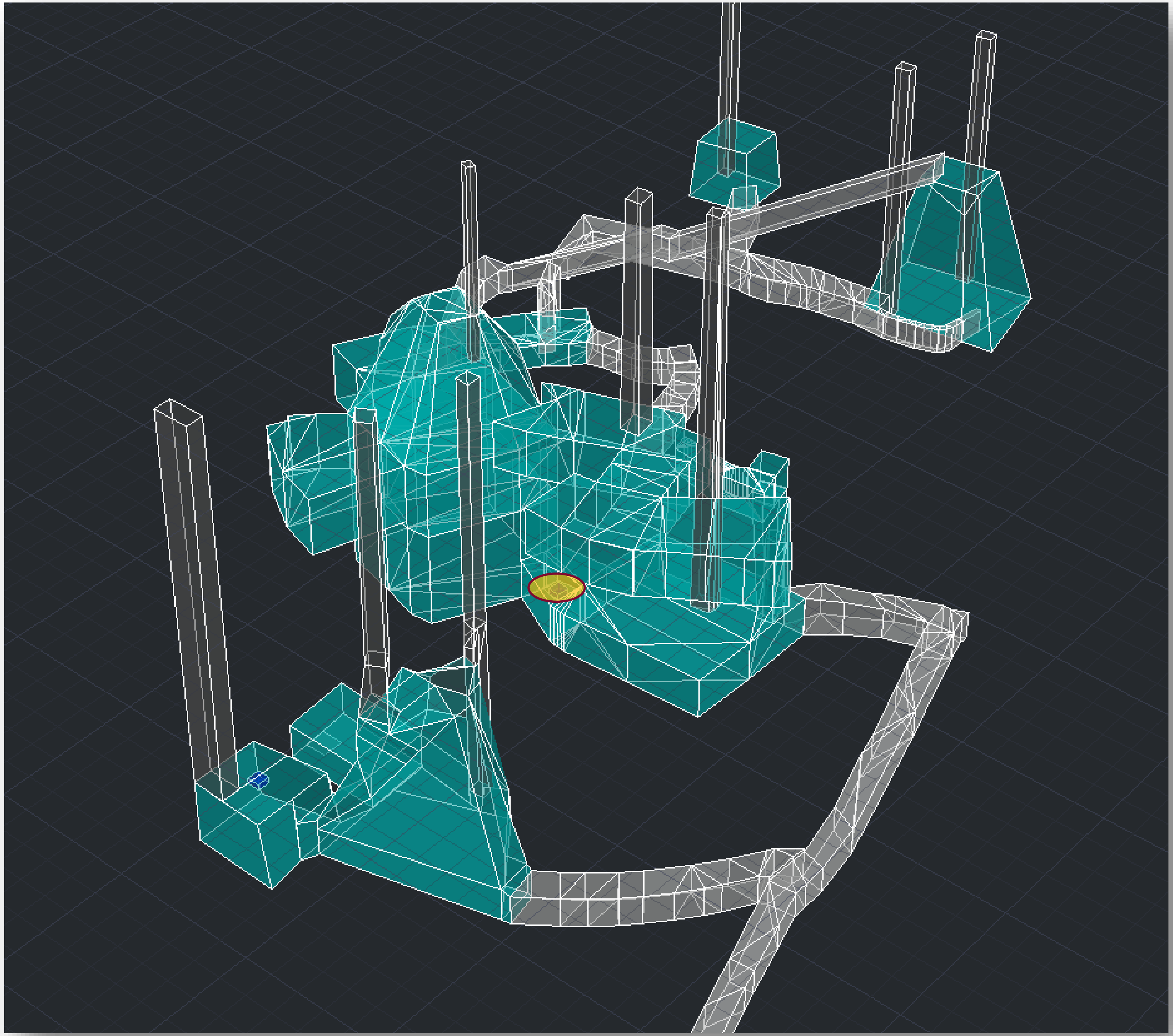

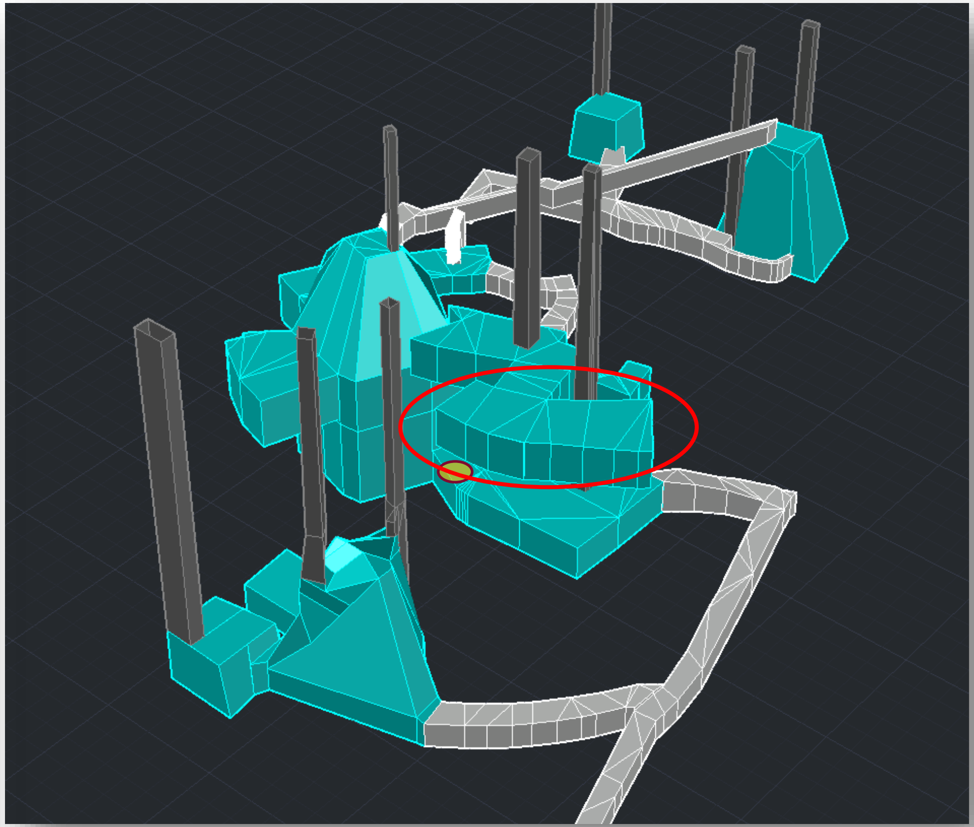

Pool site    Target region

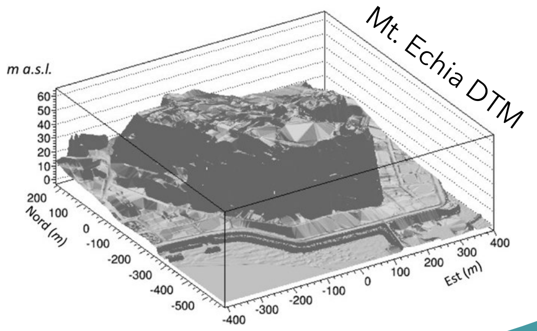

# COMPUTIZED TECHNIQUES

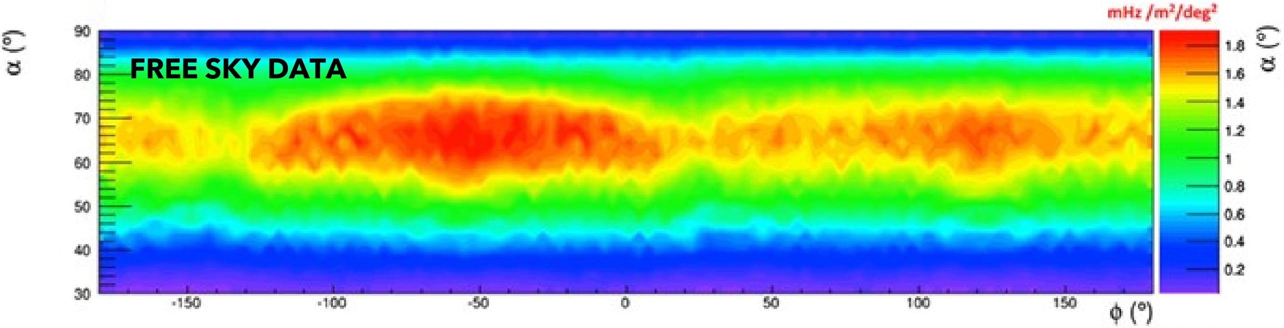


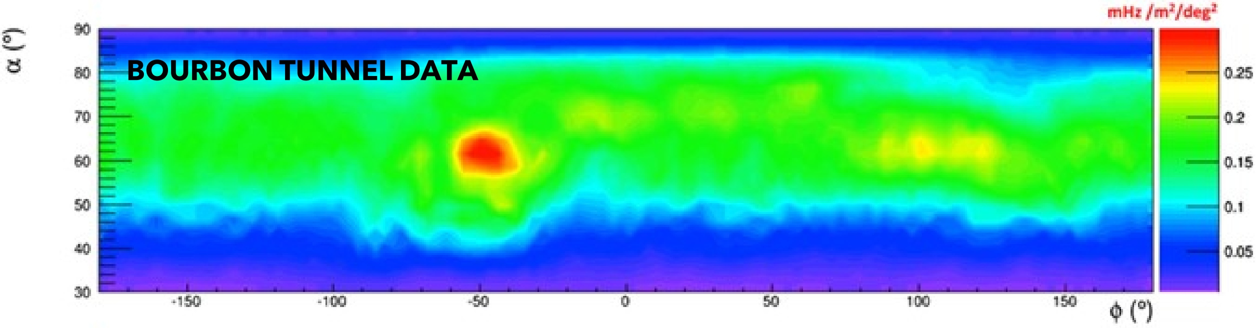


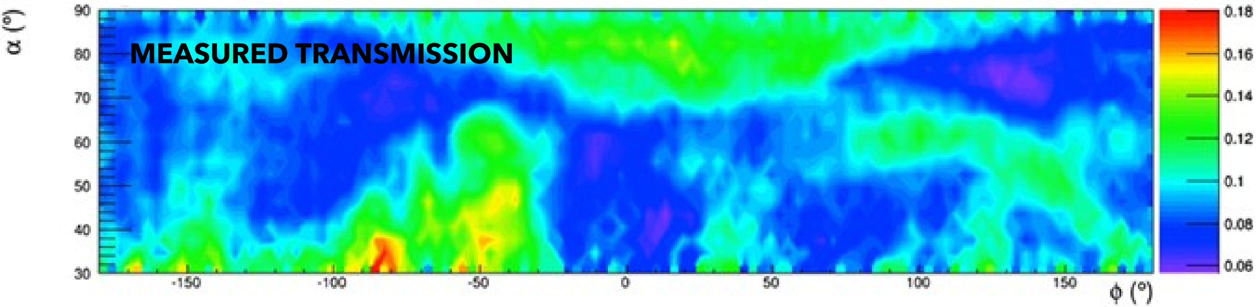


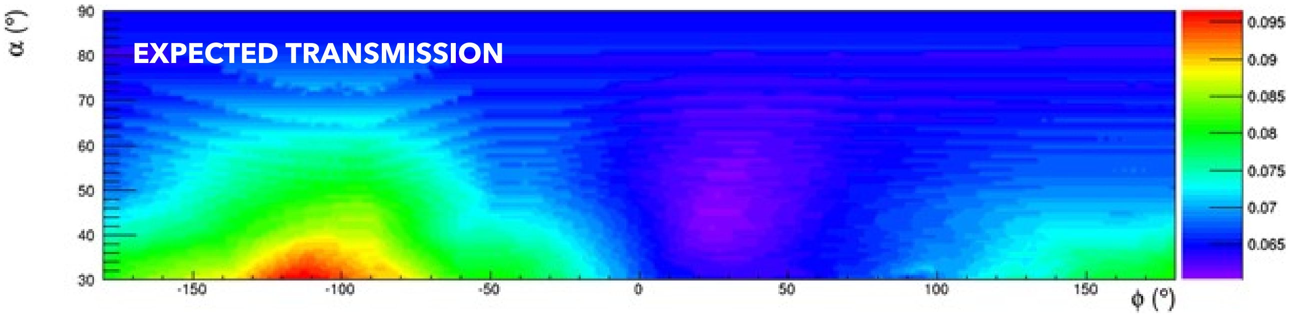


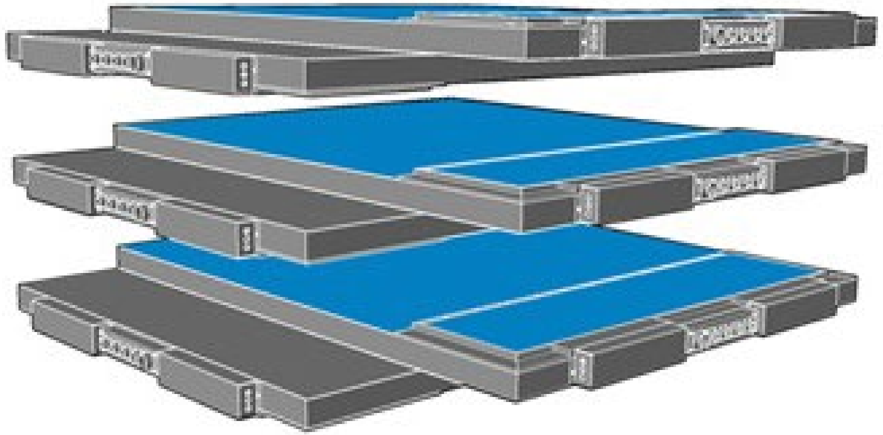

The MURAY detector, used to make this measurement, consists of a vertical sequence of three 1 $m^2$ XY-planes, mounted horizontally on a support (not shown) and evenly spaced in the vertical direction (Z axis).

The XY-planes are spaced from each other by 25 cm and the angular aperture is 60°.

# COMPUTIZED TECHNIQUES

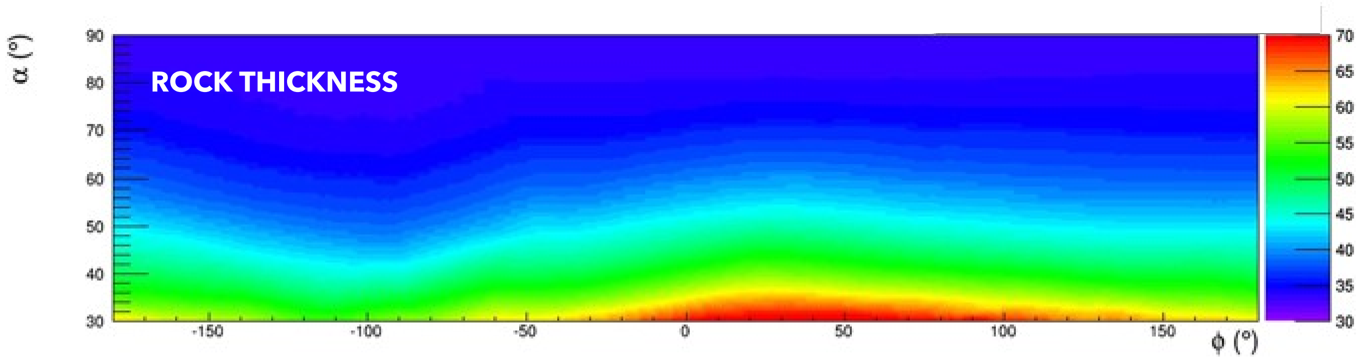


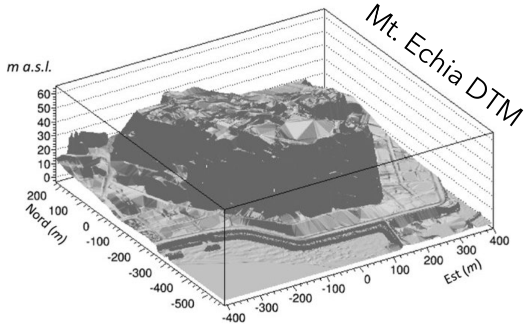


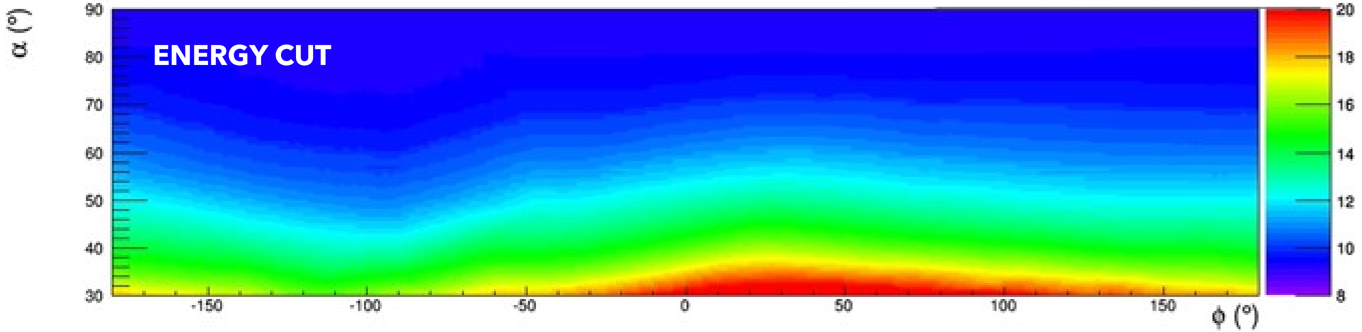


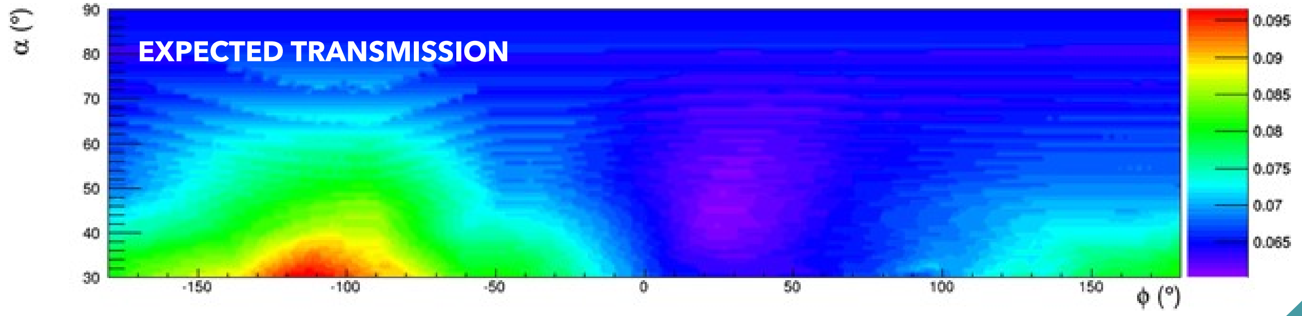


$$T_{exp}(\theta,\varphi) = \frac{\int_{E_{min}}^{\infty} i(\theta,\varphi,E_\mu)\,dE_\mu}{\int_{E_0}^{\infty} i(\theta,\varphi,E_\mu)\,dE_\mu}$$

# COMPUTIZED TECHNIQUES

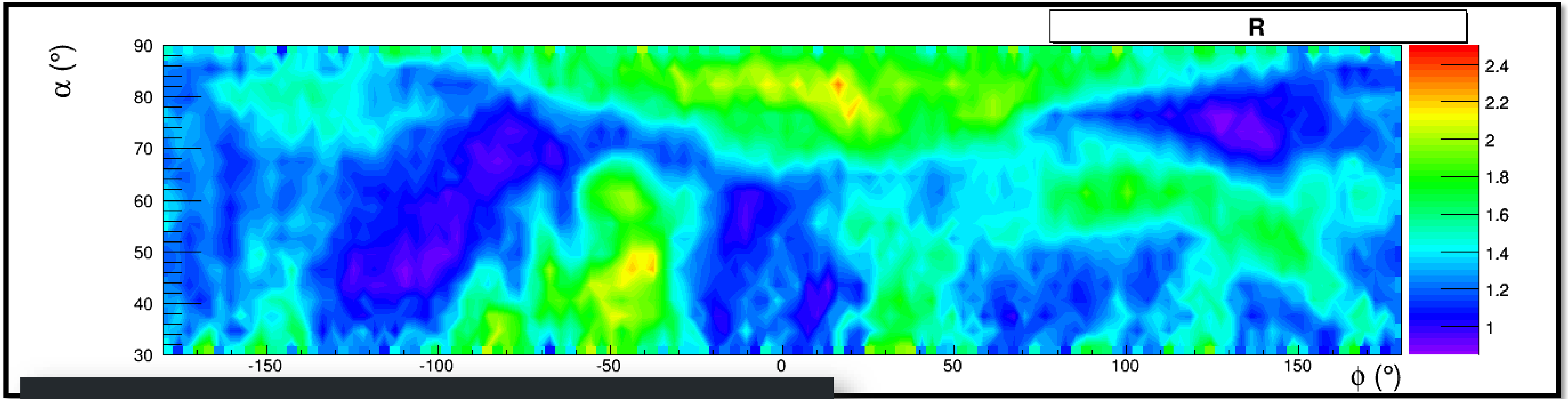


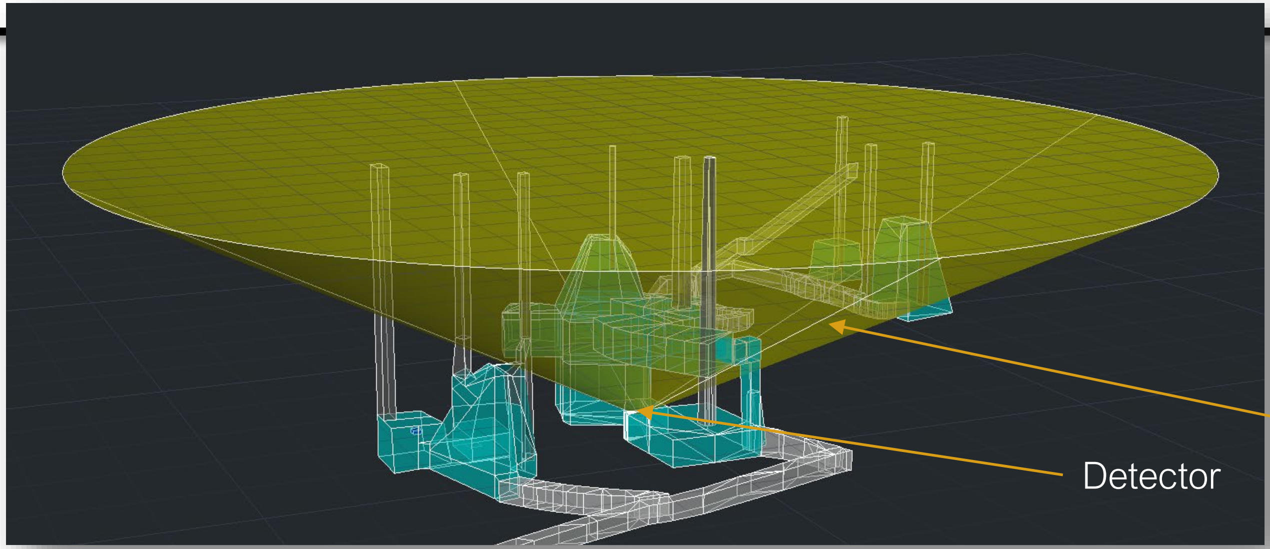


Acceptance cone of the detector

$$R(\theta,\varphi) = \frac{T(\theta,\varphi)}{T_{exp}(\theta,\varphi)}$$

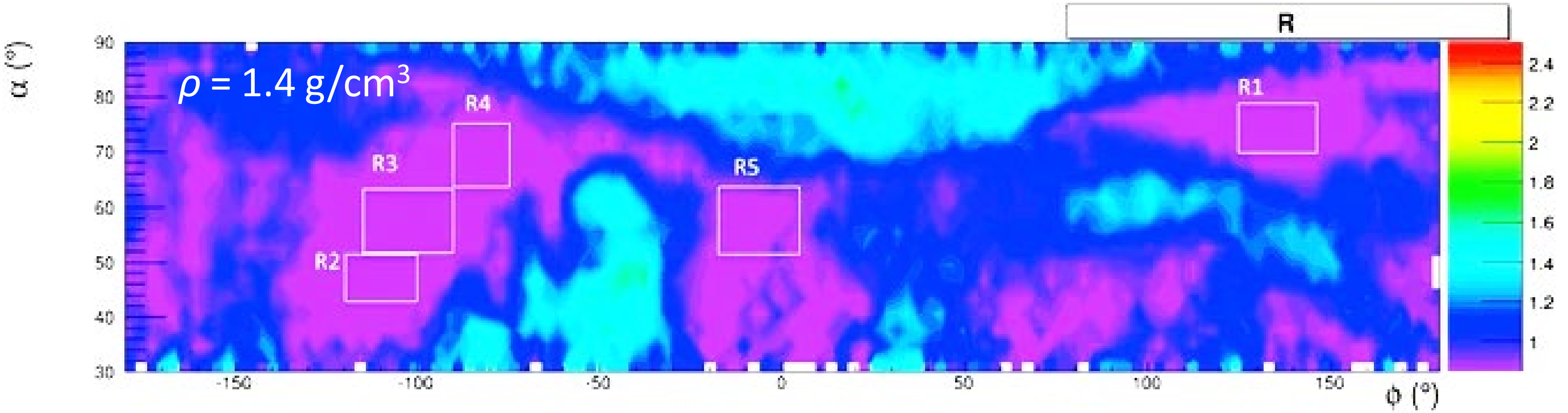


$\rho$ = 1.71 g/cm$^3$

$\sigma_\rho$ = 0.013 g/cm$^3$

$\sigma_m$ = 0.04 g/cm$^3$

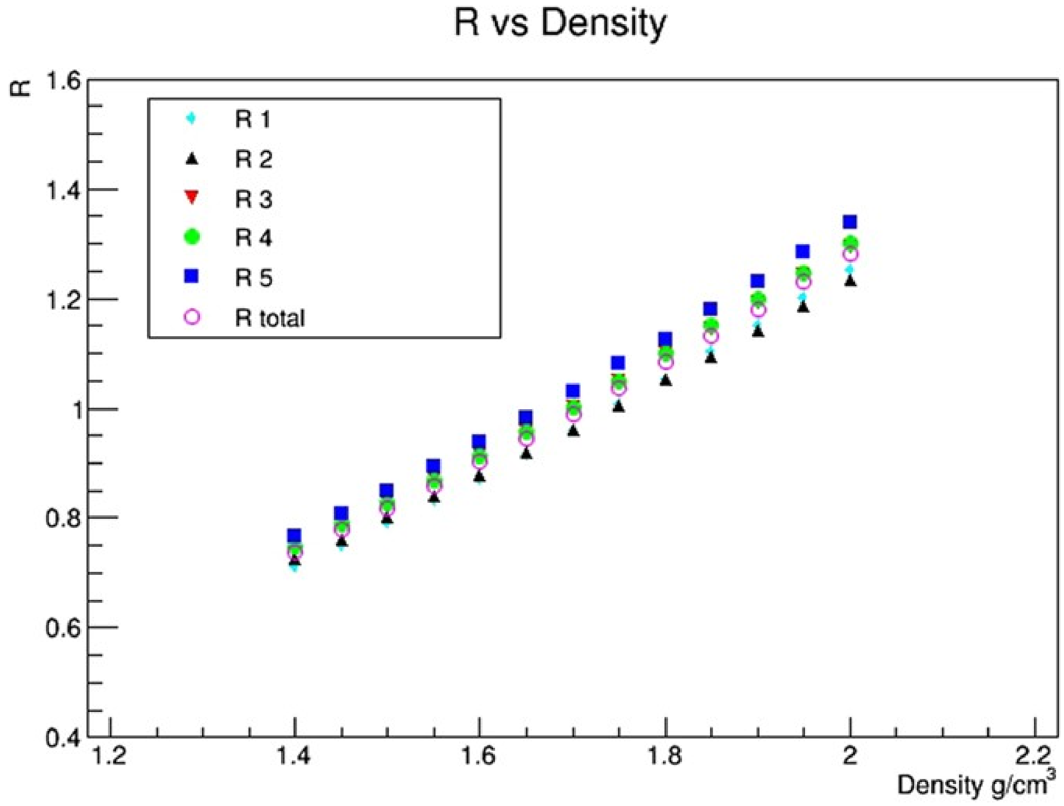


The density is measured using angular regions where minimum values of the transmission are found.

Different scatter plots of the relative transmission R are produced varying the density and the relative transmission values of the control regions are plotted in function of the density.

In these regions, where there are no cavities, the expected value of the relative transmission must be **R = 1**.

# COMPUTIZED TECHNIQUES

The red line represents the outline of the simulated muography starting from the CAD model.

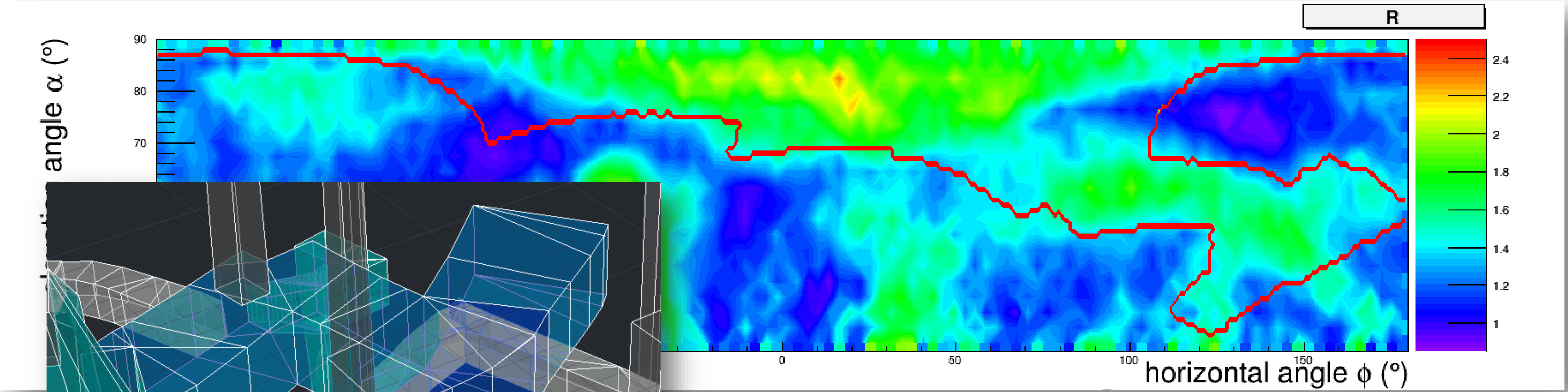


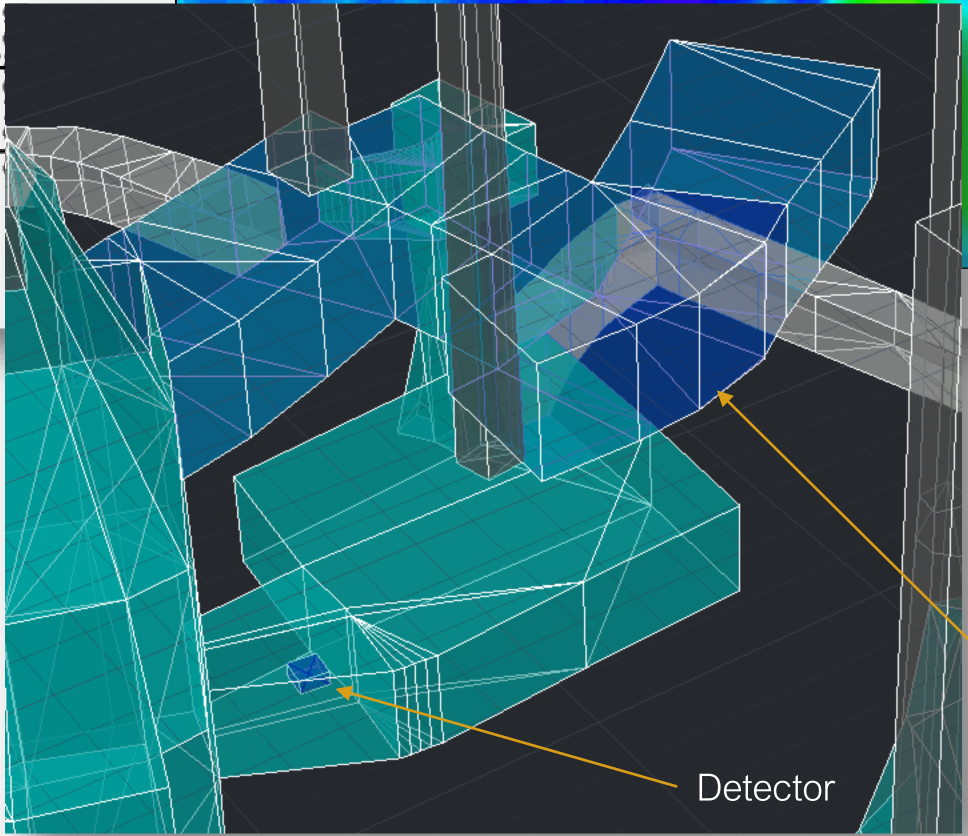


There is a very good agreement between the obtained image and the simulated one. The parts that do not overlap depend on both structural factors of the room and a CAD model that does not perfectly reproduce the original.

Known cavity corresponding to the red line overlaid to the muography

# COMPUTIZED TECHNIQUES

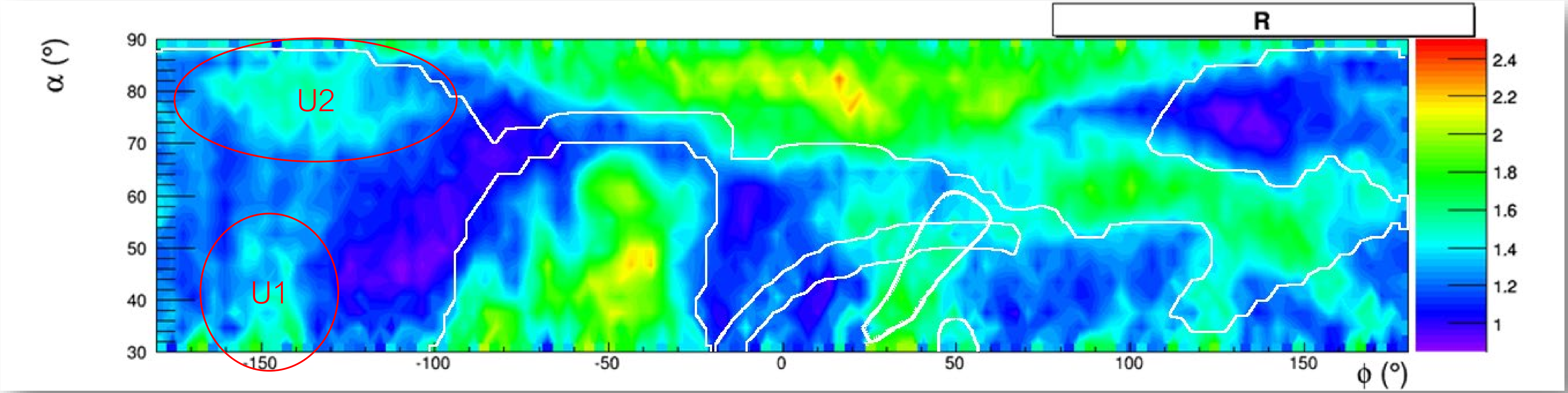


We simulated all known structures. The aim is to trace the green regions of the muography (that correspond to signals) and all green that rest uncovered might be unknown cavities.

The regions U1 and U2 aren't in the CAD model. Their signal correspond to unknown cavities.

In order to understand the hidden structures that generates these signals, we decided to make a new muography from a point of view closer to these hypothetical structures. The so-called tank site is easily accessible and large enough to install the detector.

# COMPUTIZED TECHNIQUES

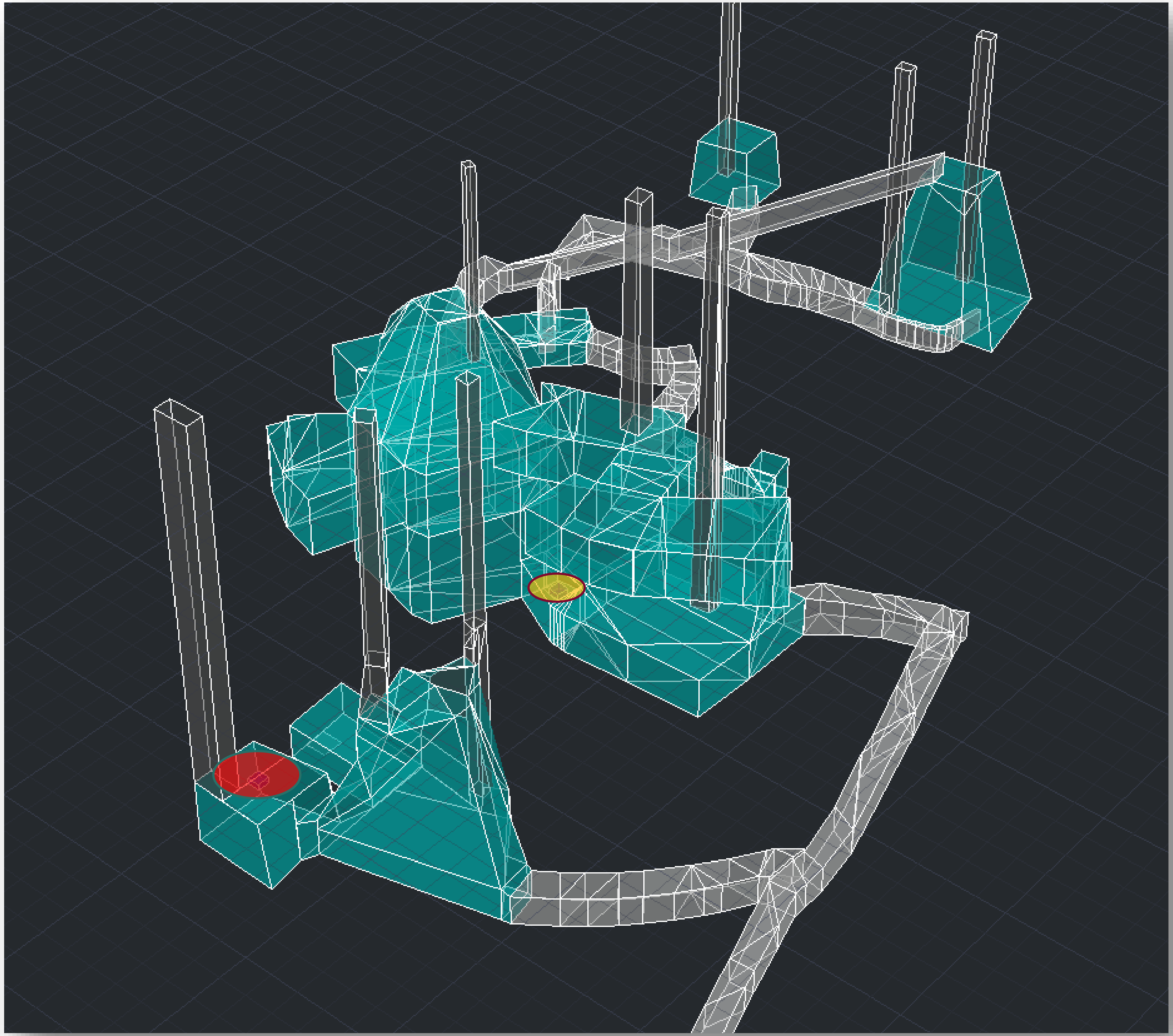

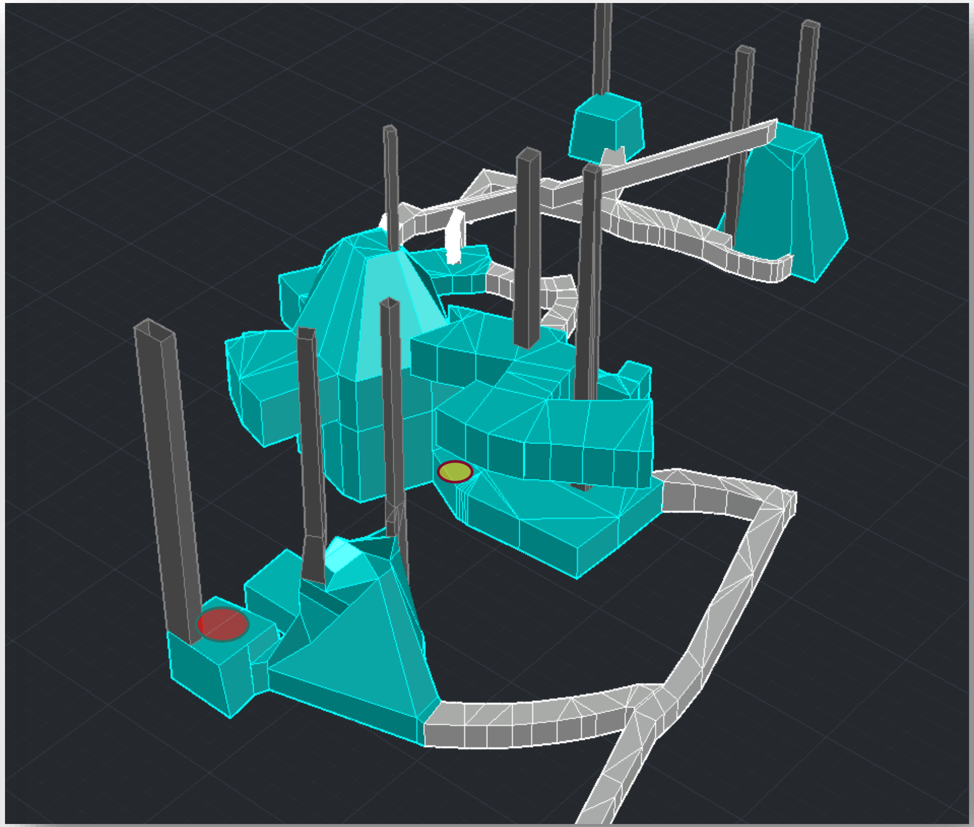

Pool site    Tank site

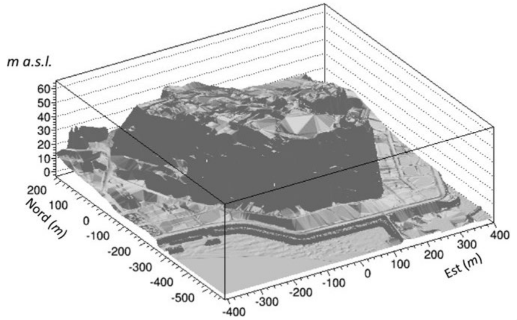

# COMPUTIZED TECHNIQUES

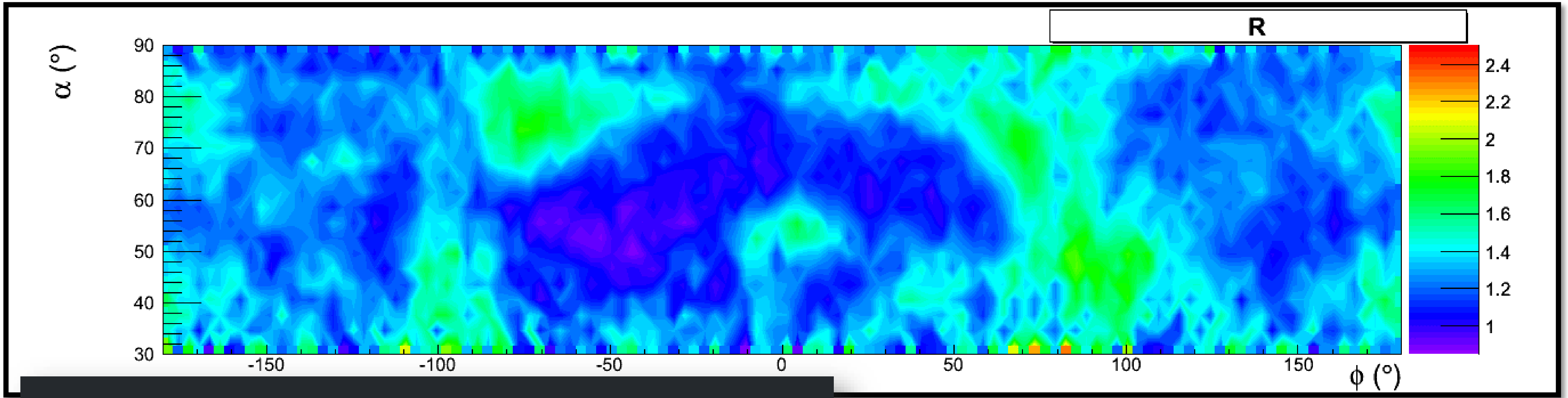


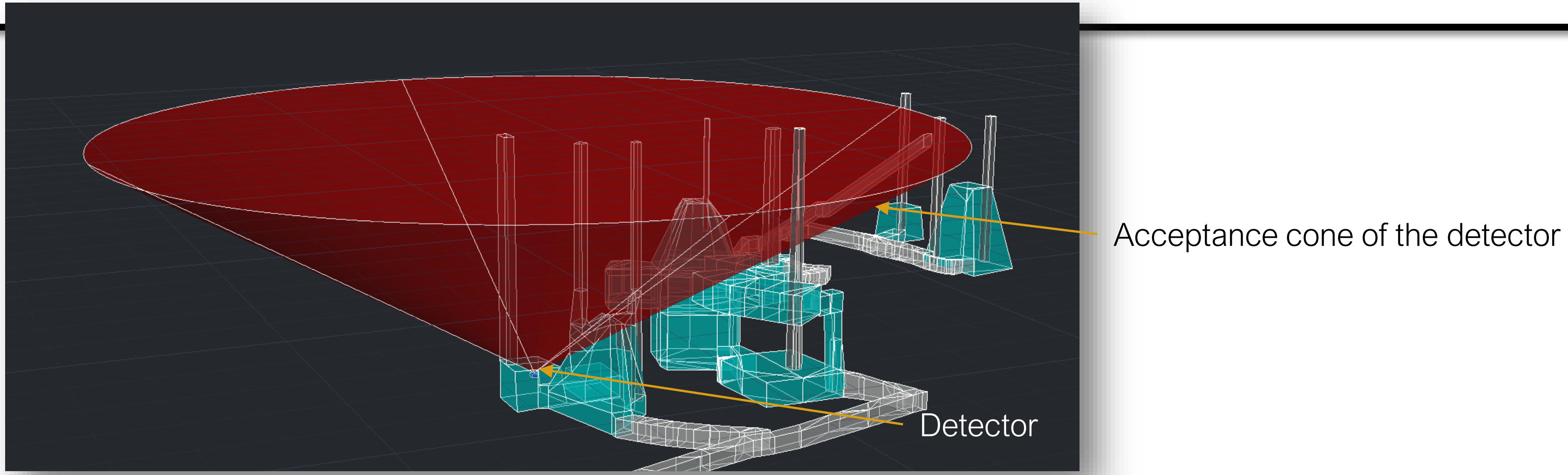

# COMPUTIZED TECHNIQUES

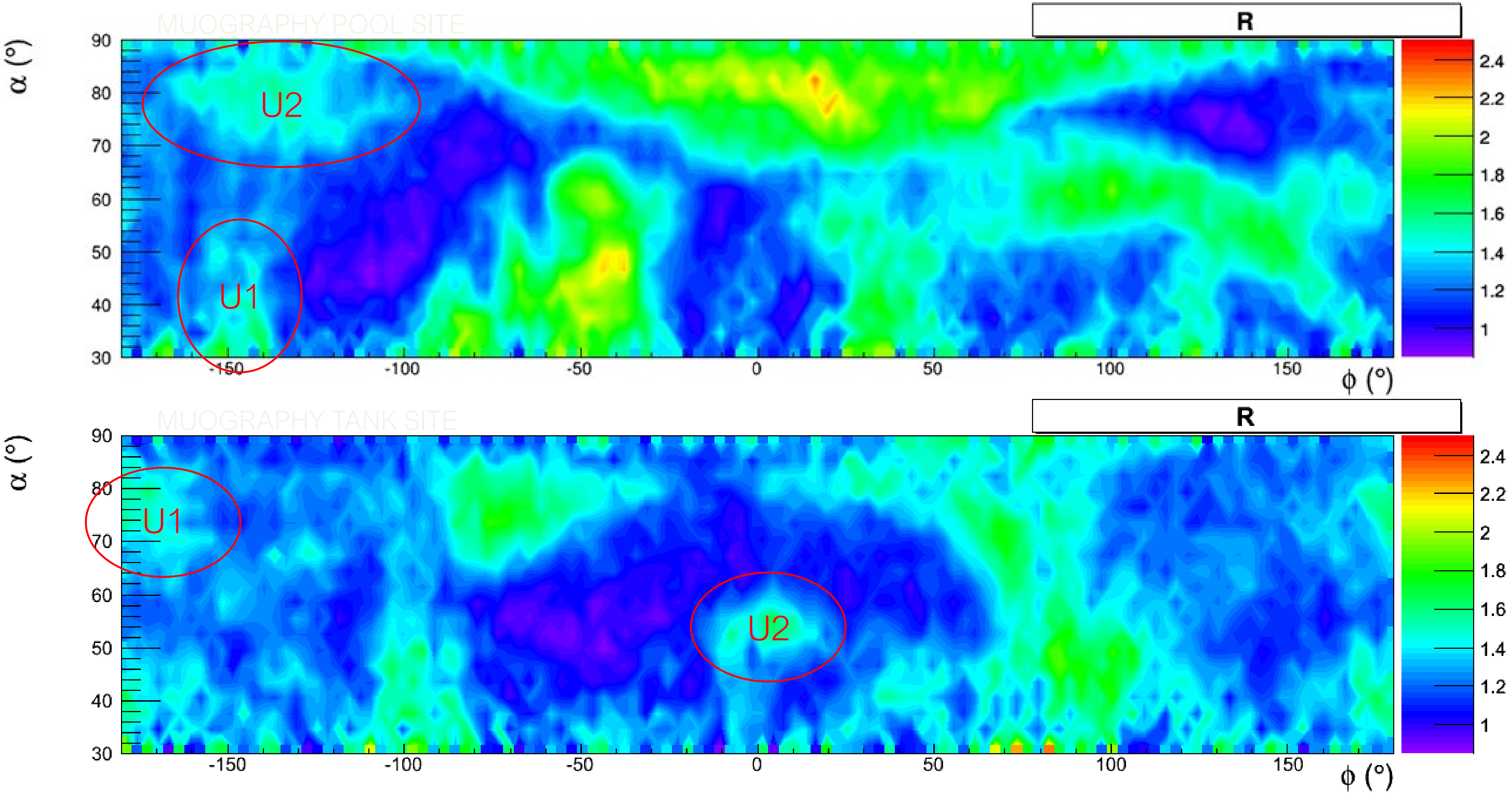

# COMPUTIZED TECHNIQUES

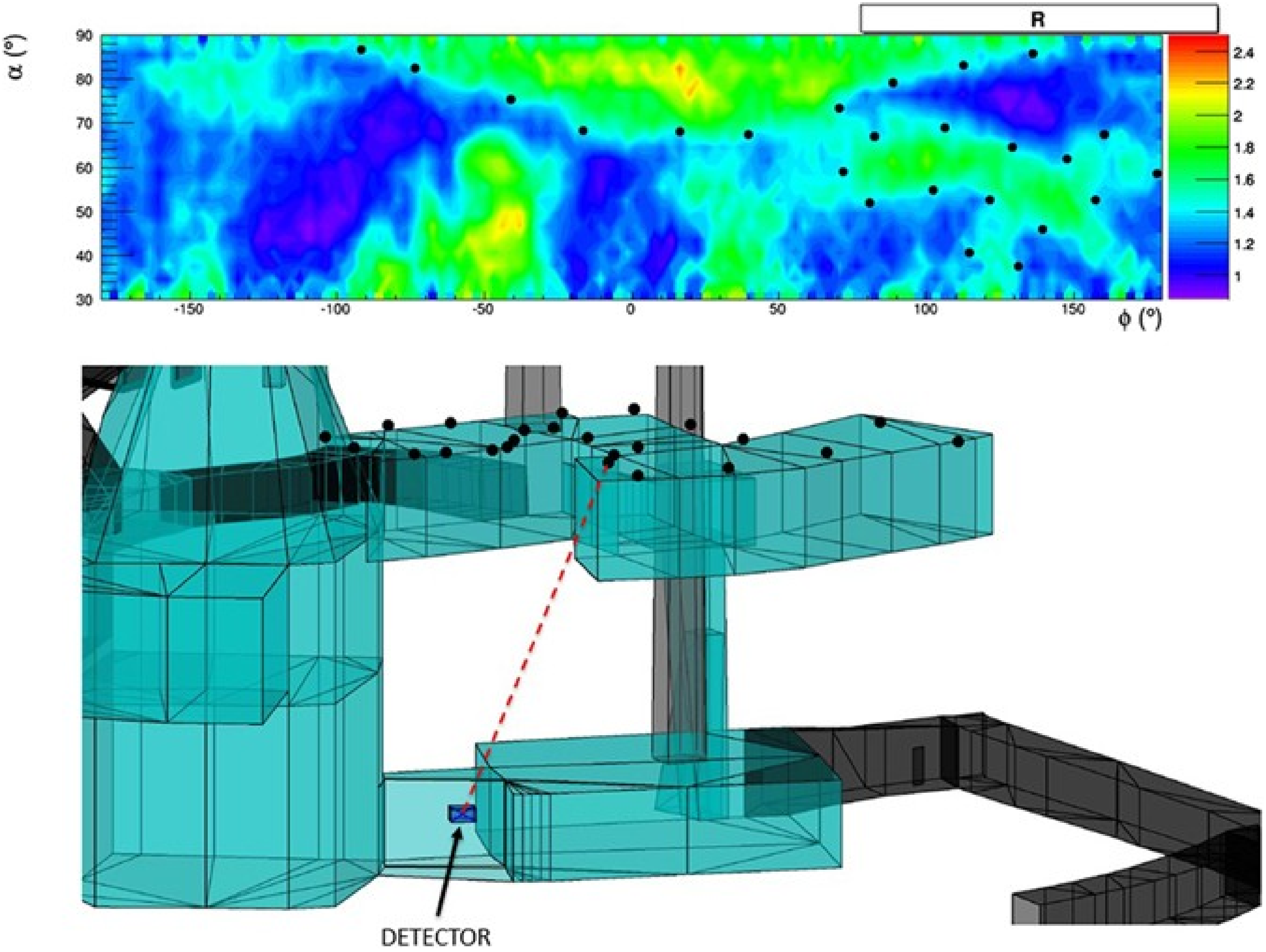


The muography can be used to reshape the CAD model with a new cloud of points that better match with the measured chamber.

This geometrical methods has inspired a 3D reconstruction method that uses multiple muographies to locate and to give a shape to measured signals, even if they are unknown.

# COMPUTIZED TECHNIQUES

Wanting to try to give shape to the environments identified, we proceed with a focusing method. In this example, cubic chamber of side **L** representing the underground structure, is placed along the axis perpendicular to the detectors at a distance **d**. The whole space on the right of the detector (x > 0) has been divided in two parts to identify the zones where the limit of this region are defined by different pairs of lines. In the zone 1, the limits are defined by lines $\mathbf{r_1}$ and $\mathbf{r_4}$, and in the zone 2 by $\mathbf{r_2}$ and $\mathbf{r_3}$.

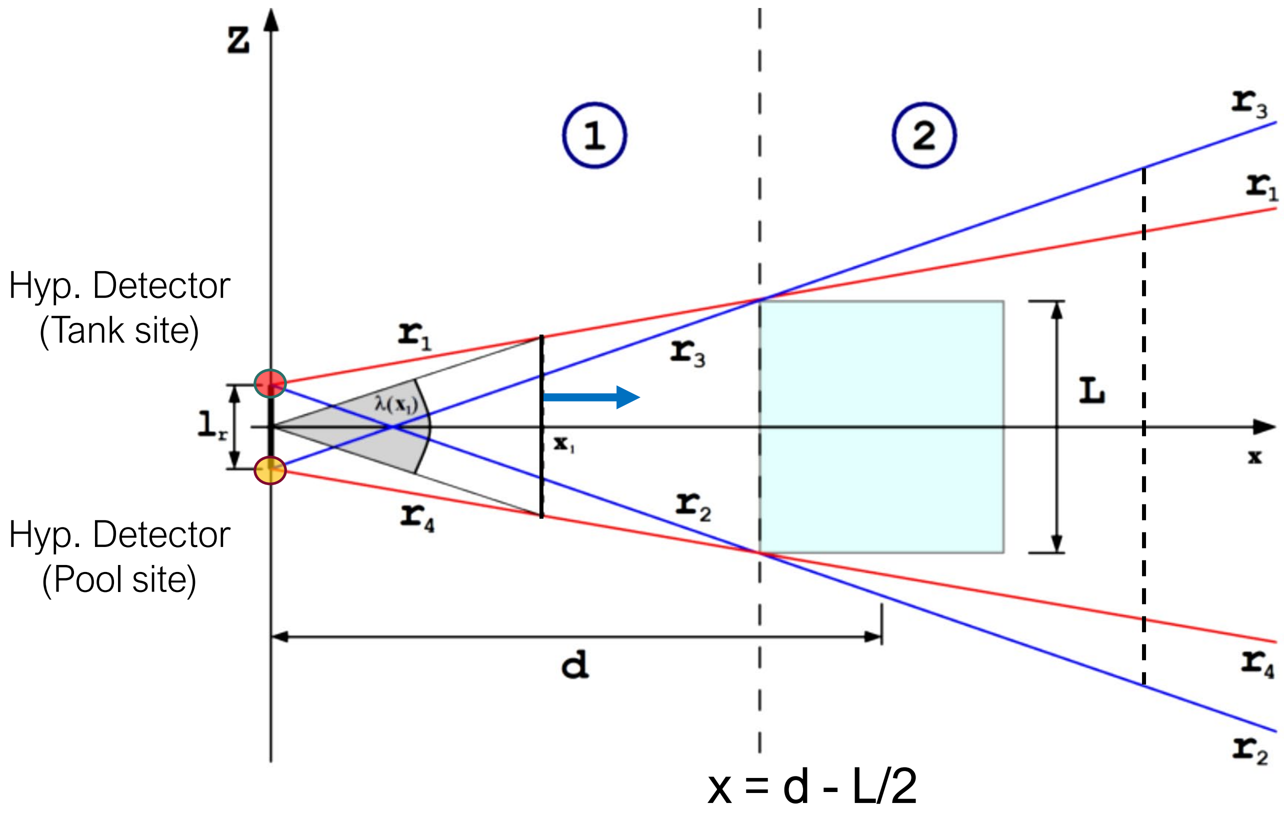


If we consider the angle **λ** subtended by these segments with respect to the mean distance between the detectors, we can see that this
angle depends on the position **x** of the selected segment, $\lambda = \lambda(x)$. So determining the minimum of $\lambda(x)$, we are able to place the chamber in the target region.

# COMPUTIZED TECHNIQUES

I the three-dimensional space we have to detetrmine the minimum in both Z-view and Y-view

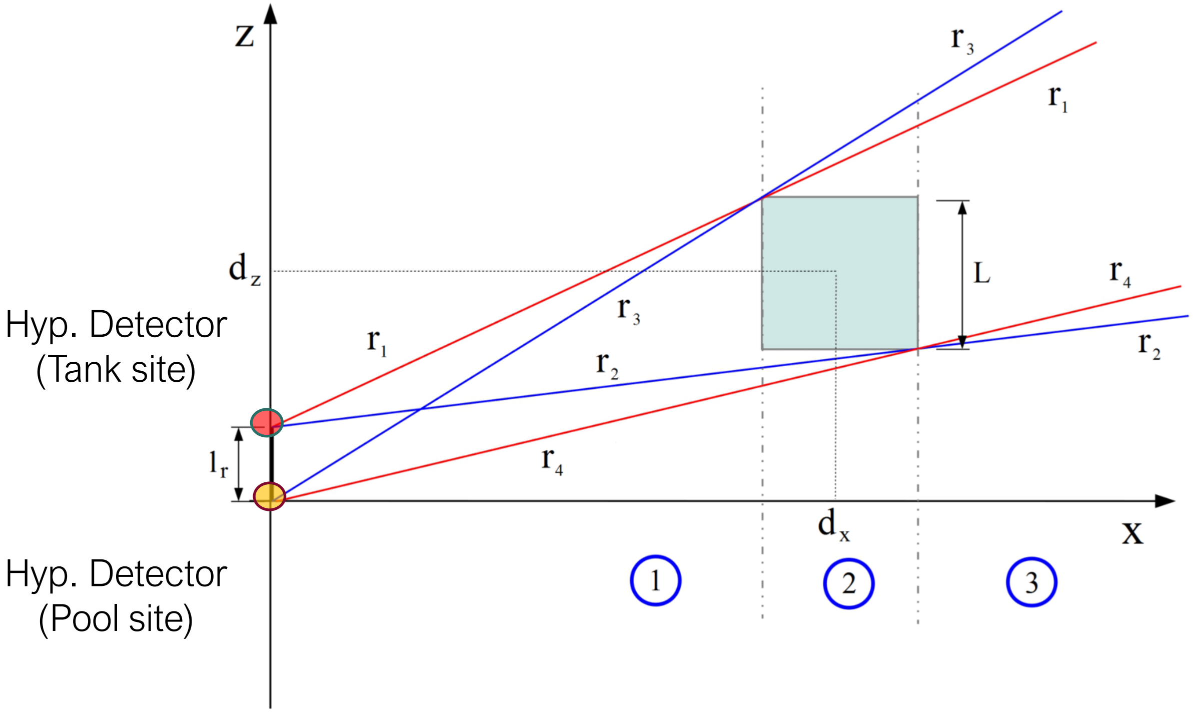


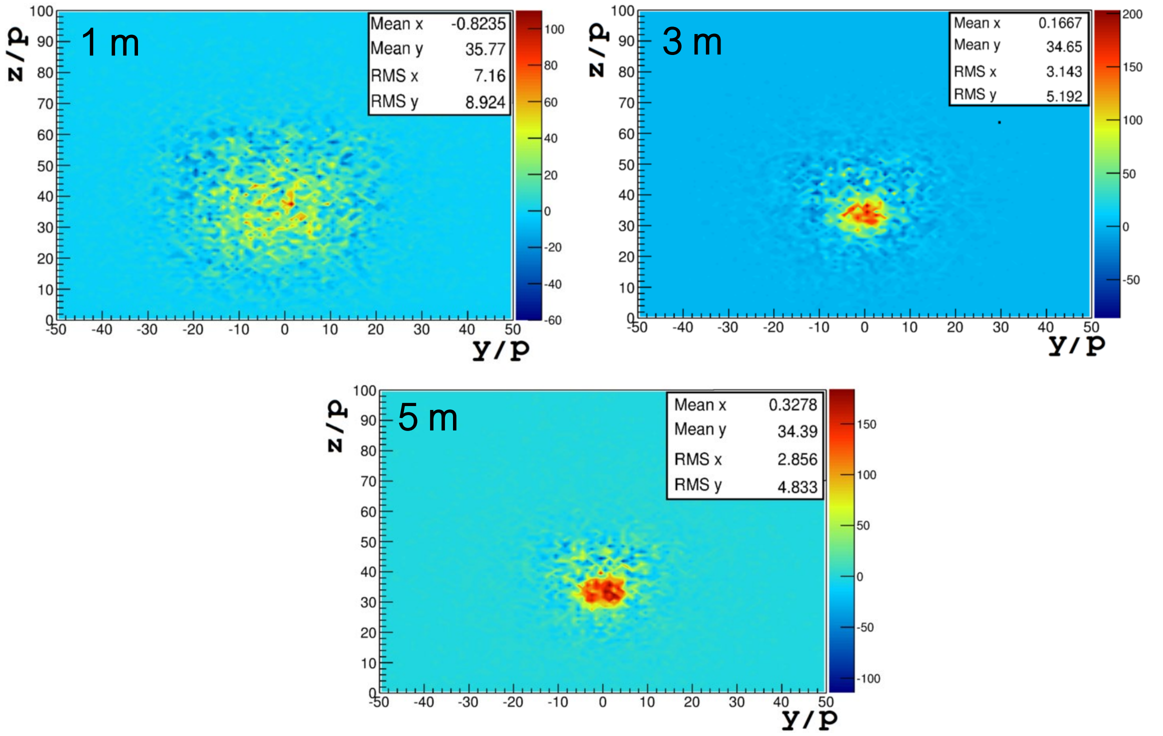


The focusing distance produce different reconstruction of the object, making it more and more defined as the distance of the plane in which the structure is located. Thus, studying the angle as a function of the distance from the YZ plane, it is possible to determine the distance on the x axis and place the object in an appropriate way within the target region.

# COMPUTIZED TECHNIQUES

I the three-dimensional space we have to detetrmine the minimum in both Z-view and Y-view

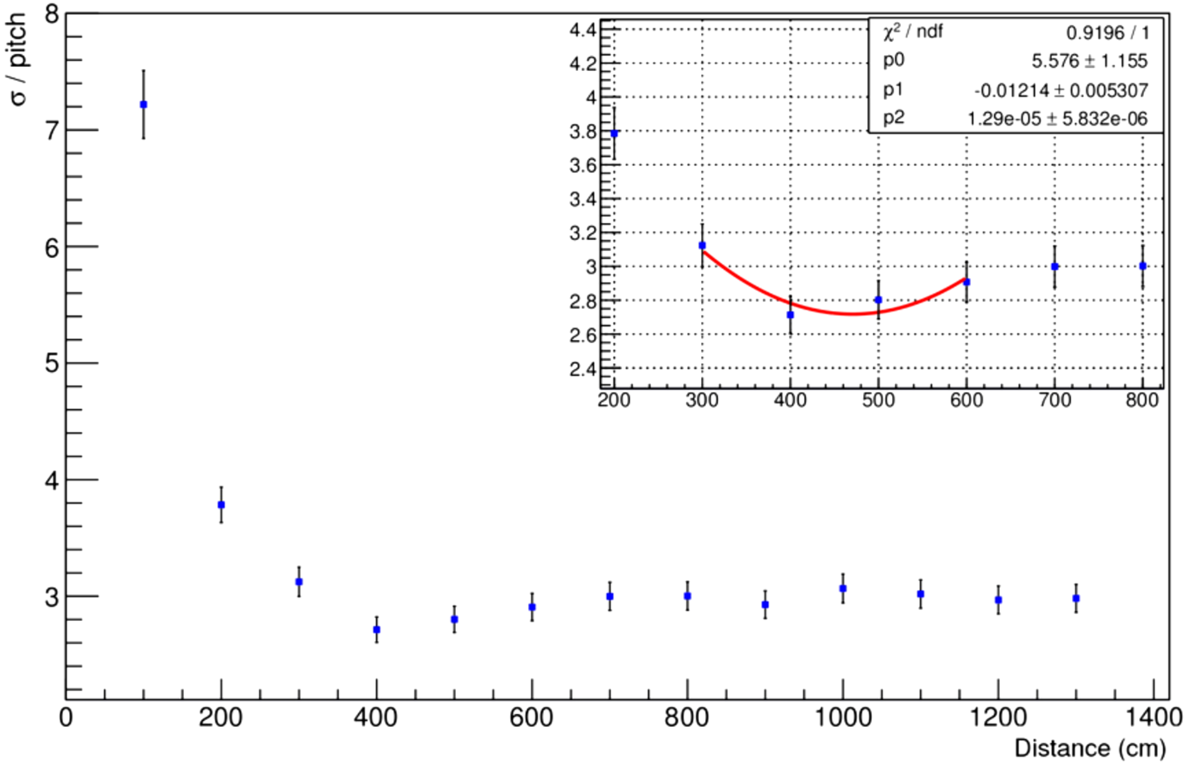


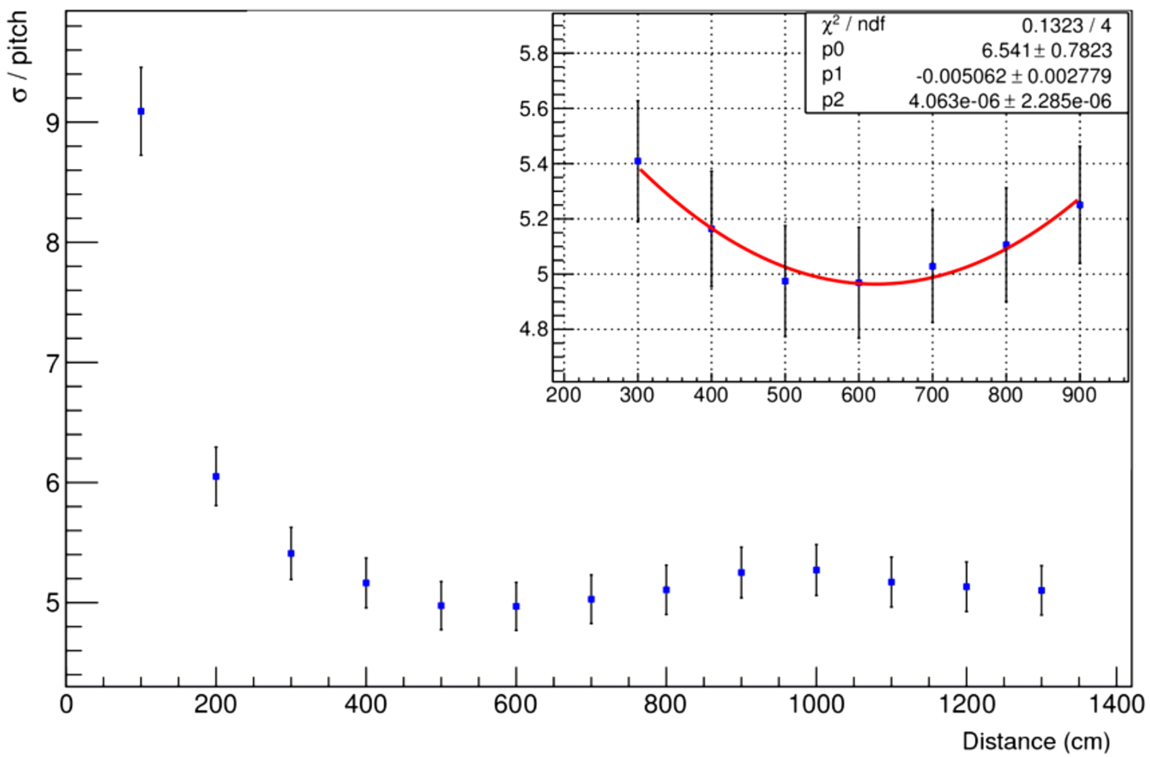


The focusing distance produce different reconstruction of the object, making it more and more defined as the distance of the plane in which the structure is located. Thus, studying the angle as a function of the distance from the YZ plane, it is possible to determine the distance on the x axis and place the object in an appropriate way within the target region.

# COMPUTIZED TECHNIQUES

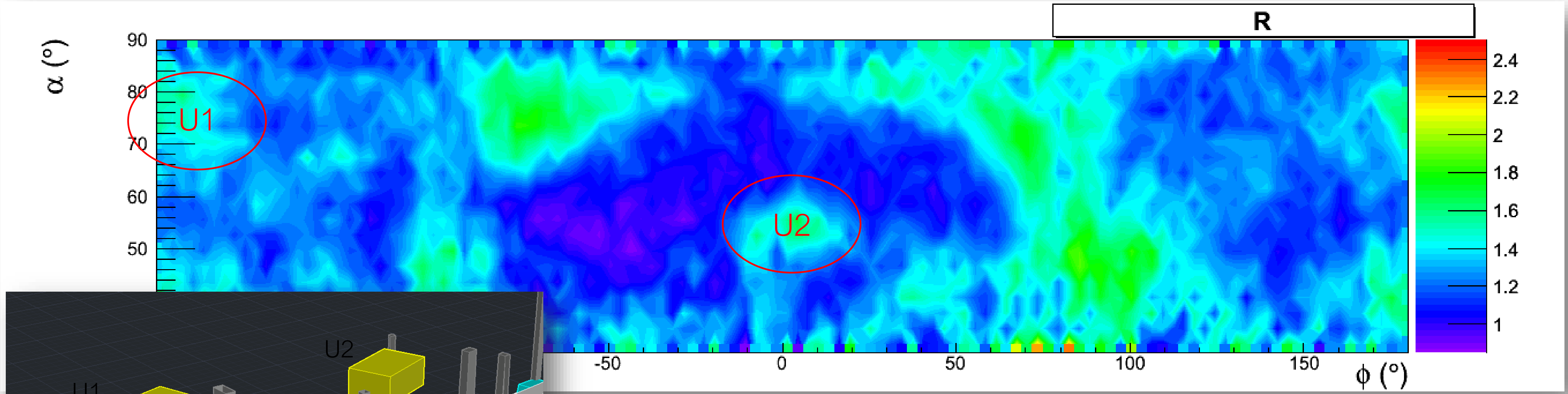


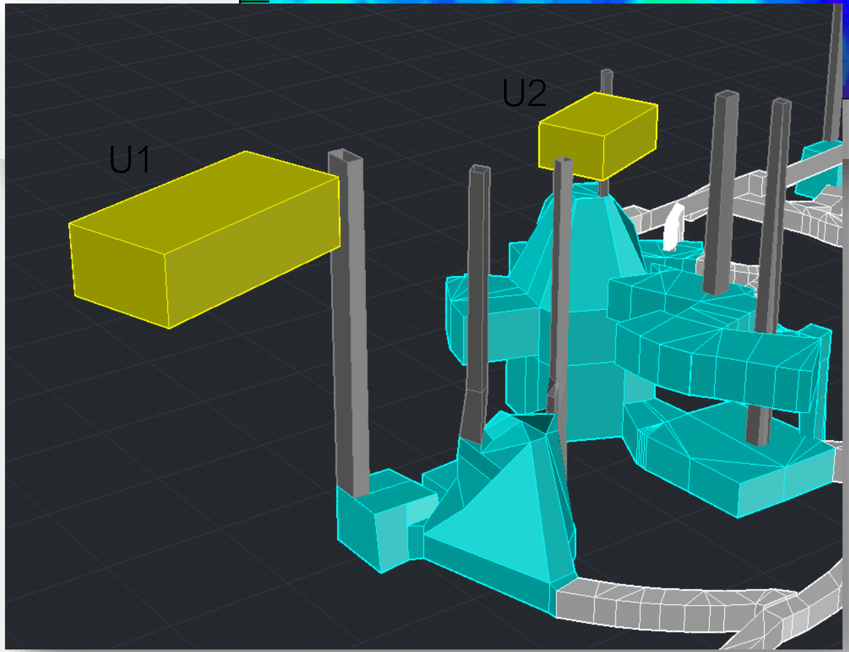


A corresponce in the regions U1 and U2 in both muographies, implies the existence of two large empty spaces, plausible just below the top of the hill.

According to experts, chambers like this (extention and position) can not be there and they have no signs of their presence. The urban condition of this zone of the city is well known.

# COMPUTIZED TECHNIQUES

To have a further confirmation of the muographic signals seen at the pool and at the tank, we decided to use a second detector with tilting capacity. This allows us to aim directly at the target region by maximizing the area exposed to the muon flux in the direction of the target region.

The MIMA detector has tilting capacity and some feature in common with the MURAY detector. It is compact and portable, so it can be easily installed even in confined spaces.

These characteristics have allowed us to carry out a further muography in order to surround the target region, even if not on all sides.

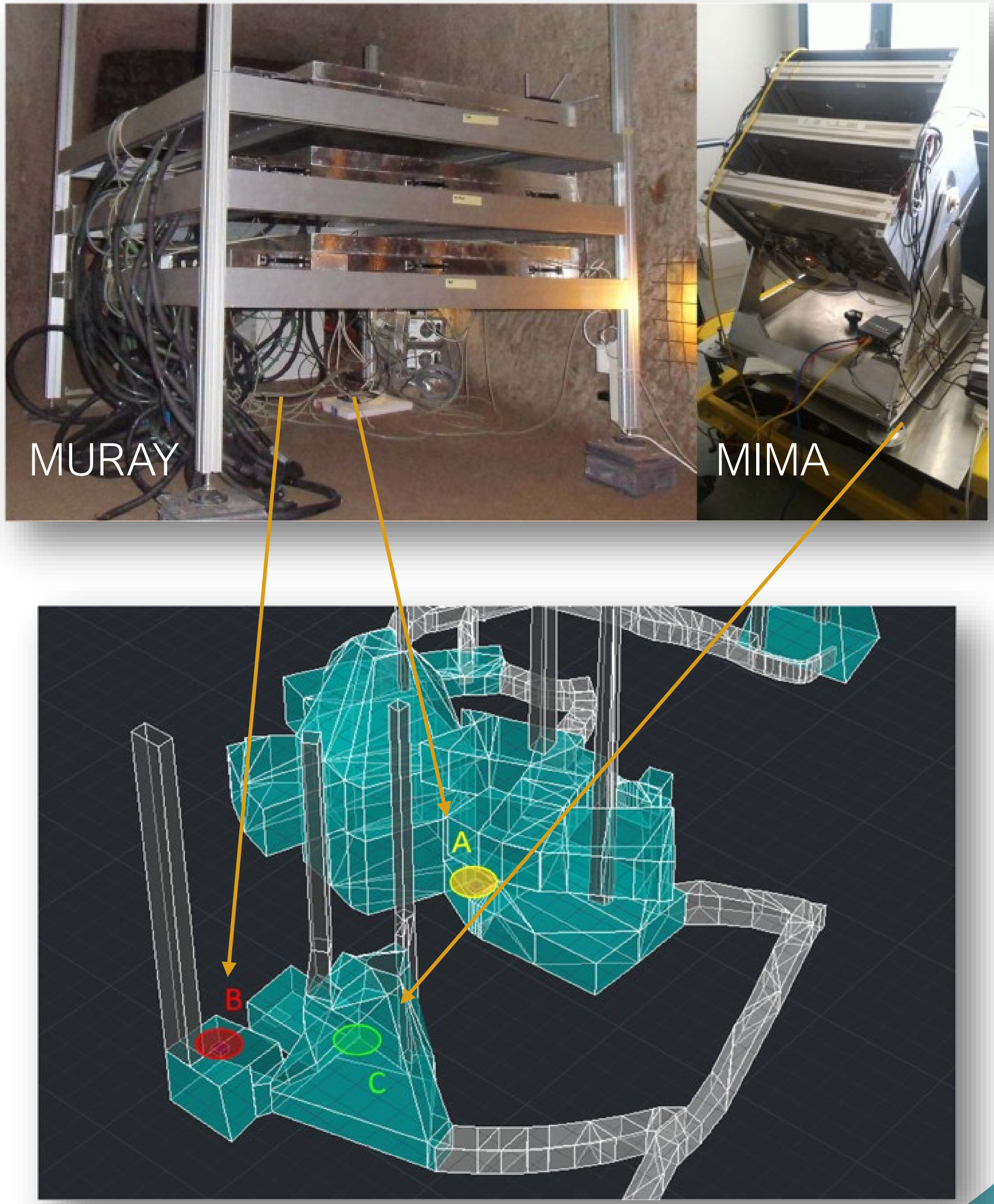

# COMPUTIZED TECHNIQUES

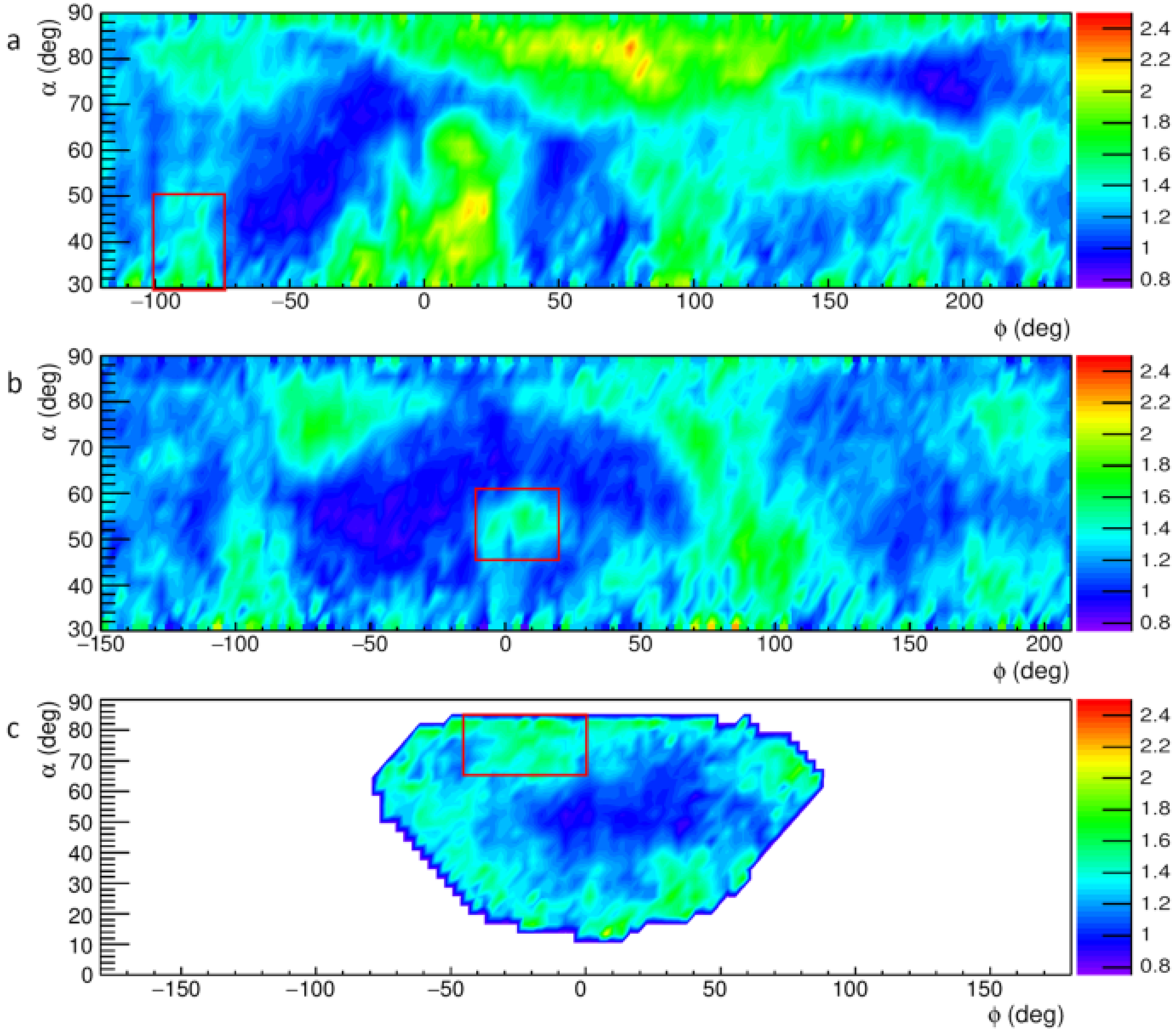


Using an algorithm that scans for signals, imposing an arbitrary minimum threshold value, we are able to determine the signals that intersect on all three muographs. this produces different combinations which do not necessarily correspond to cavities. For example, the algorithm also matches the signals used previously and which in reality may not correspond to environments with that extension and that depth.

A reasonable combination of signals in angular coincidence between the three muographs taken from the three different sites is given by the areas delimited by red rectangles. these three signals seen from the three points of view could correspond to a single environment.

# COMPUTIZED TECHNIQUES

a

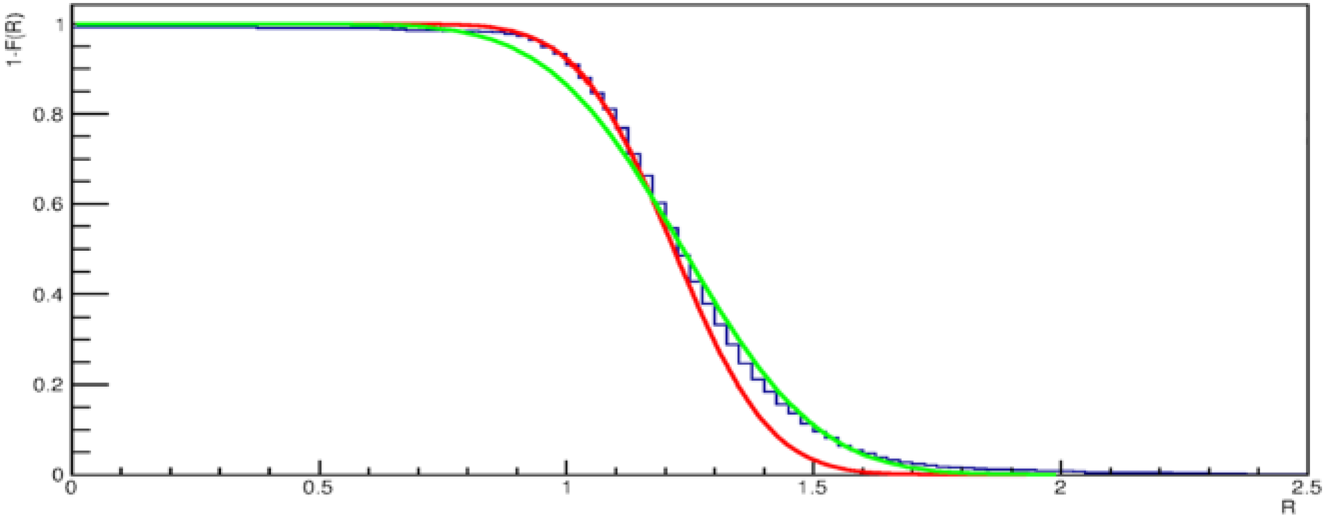


b

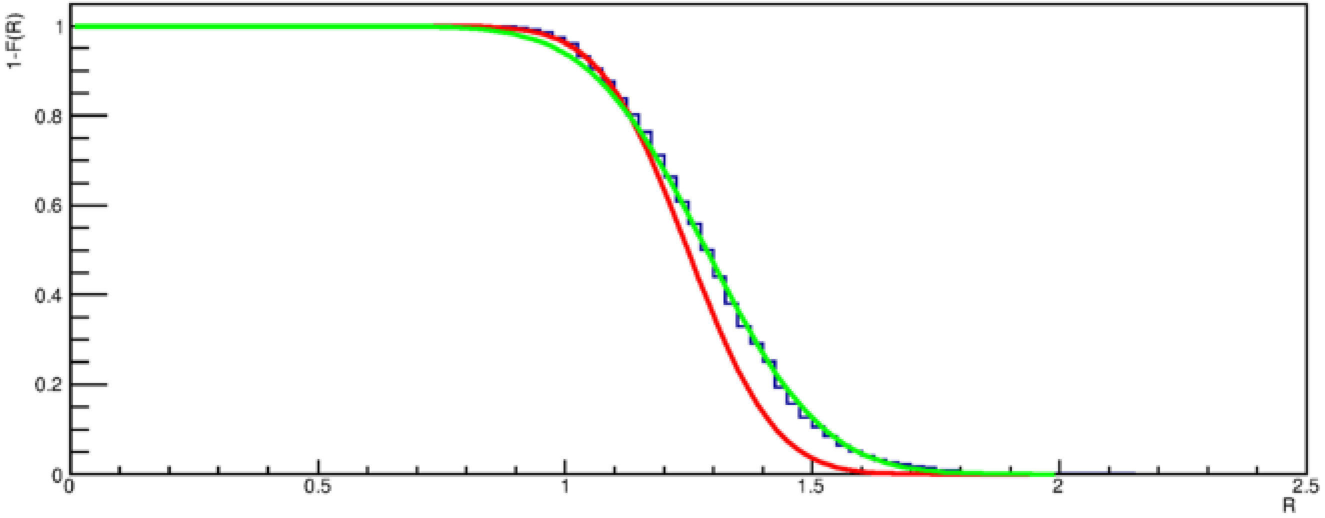


The distribution of the relative transmission R given in each muography was interpreted as the sum of two components, one corresponding to transmission through rock without voids and another corresponding to transmission through rock with voids.

Using the cumulative distributions of the relative transmission of each muography, we fit two trends as hypotesized.

The fits are shown for one of the locations of the MU-RAY muon tracker and for the MIMA muon tracker.

# COMPUTIZED TECHNIQUES

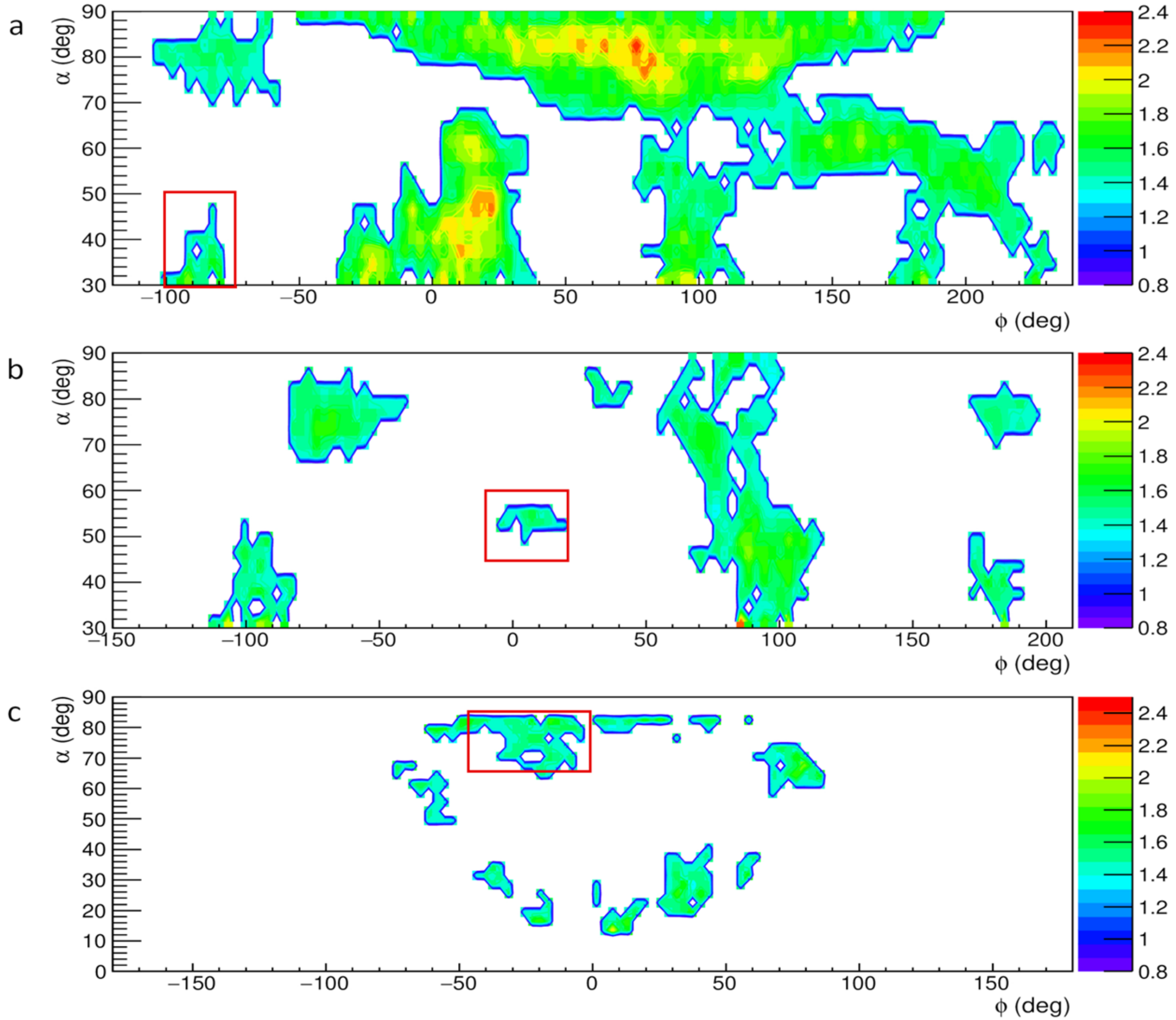


A clustering algorithm was applied to select regions with a relative transmission R above a significant threshold value, so that they could be considered as corresponding to cavities.

The component corresponding to transmission through solid rock was used to set the threshold to define the clusters corresponding to the presence of voids. This threshold was set at a value such that the probability to be a solid rock region is smaller than 2.5%. This corresponds to a value of R above **1.51** in the muographies acquired with the MURAY tracker and to a slightly different value (1.52) for the muography with the MIMA.

# COMPUTIZED TECHNIQUES

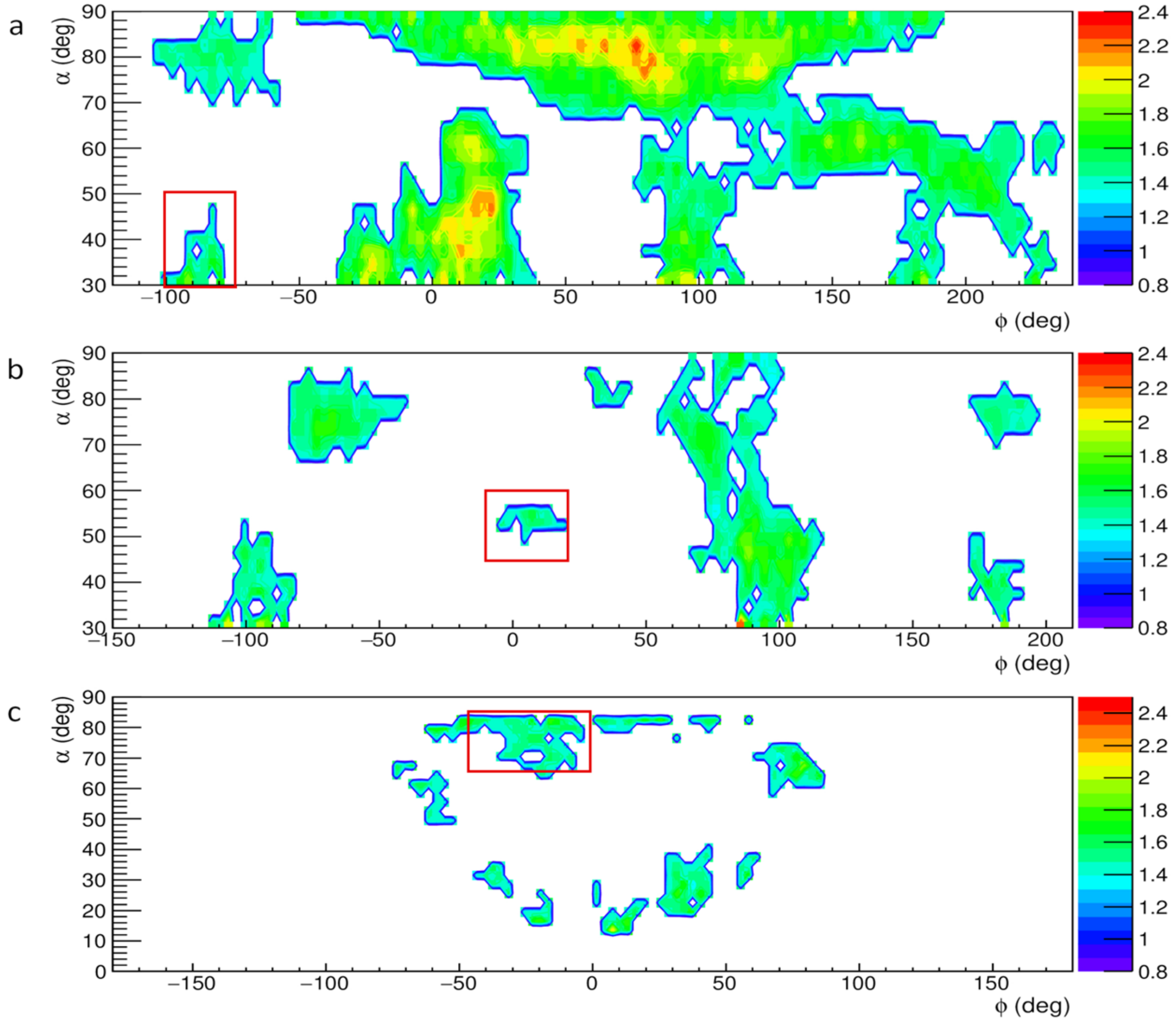


The threshold is used to search for the starting regions of the clustering algorithm. Subsequent recursive aggregation of points appearing in the 2D muography to each cluster is made by lowering progressively the threshold in R for points which are close in space to existing clusters.

Cluster reconstruction stops when no further points (close in space to an existing cluster) have a high-enough value of R (1.37 for MURAY and 1.39 for MIMA) to be associated to the cluster. In this second selection the probability for a rock filled bin to exceed the thresholds was higher (16%) but the request of proximity to a signal region ensures a low background.

# COMPUTIZED TECHNIQUES

In order to reconstruct in space the hidden cavity, we started by defining a grid of points in a cubic volume that encloses the region of space where the cavity is supposed to be, according to the angular ranges defined above. As a general criterion, **a point was considered to be located inside a cavity if in each of the three muographies it corresponds to an angular bin inside a signal cluster**.

The procedure was tested by simulating the presence of a spherical cavity with 6 m diameter, approximately located at the estimated position of the hidden cavity and having a similar size. The simulated cavity was surrounded by rock using our best estimate of density for Mt. Echia ($\rho$ = 1.71 g/cm$^3$).

The spherical shape was chosen in order to study the effects of the non optimal choice of the trackers' locations, and in particular to highlight possible ensuing asymmetries.

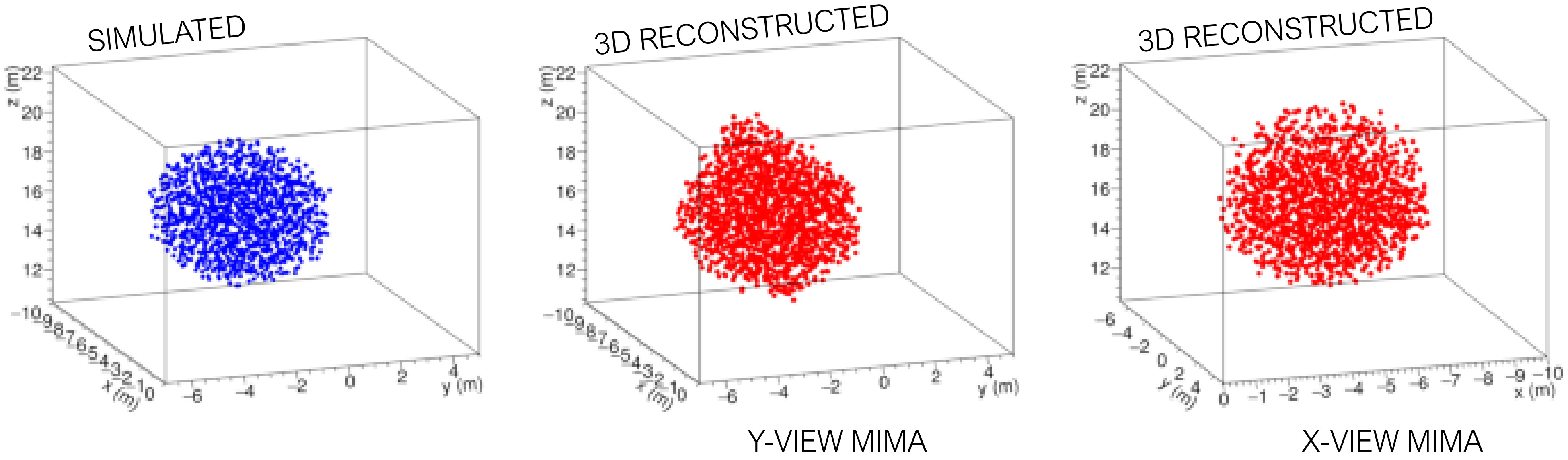

# COMPUTIZED TECHNIQUES

With this procedure we 3D reconstruct the cavity as seen by muographies. With this procedure we reconstruct the cavity seen from the muographs in 3D. Since the number of viewpoints is very low, the reconstructed form has a stereographic halo at the top, resulting slightly different from what it actually is in both shape and size.

By slicing the foreseen chamber at different height, we were able to shape it inside the CAD model.

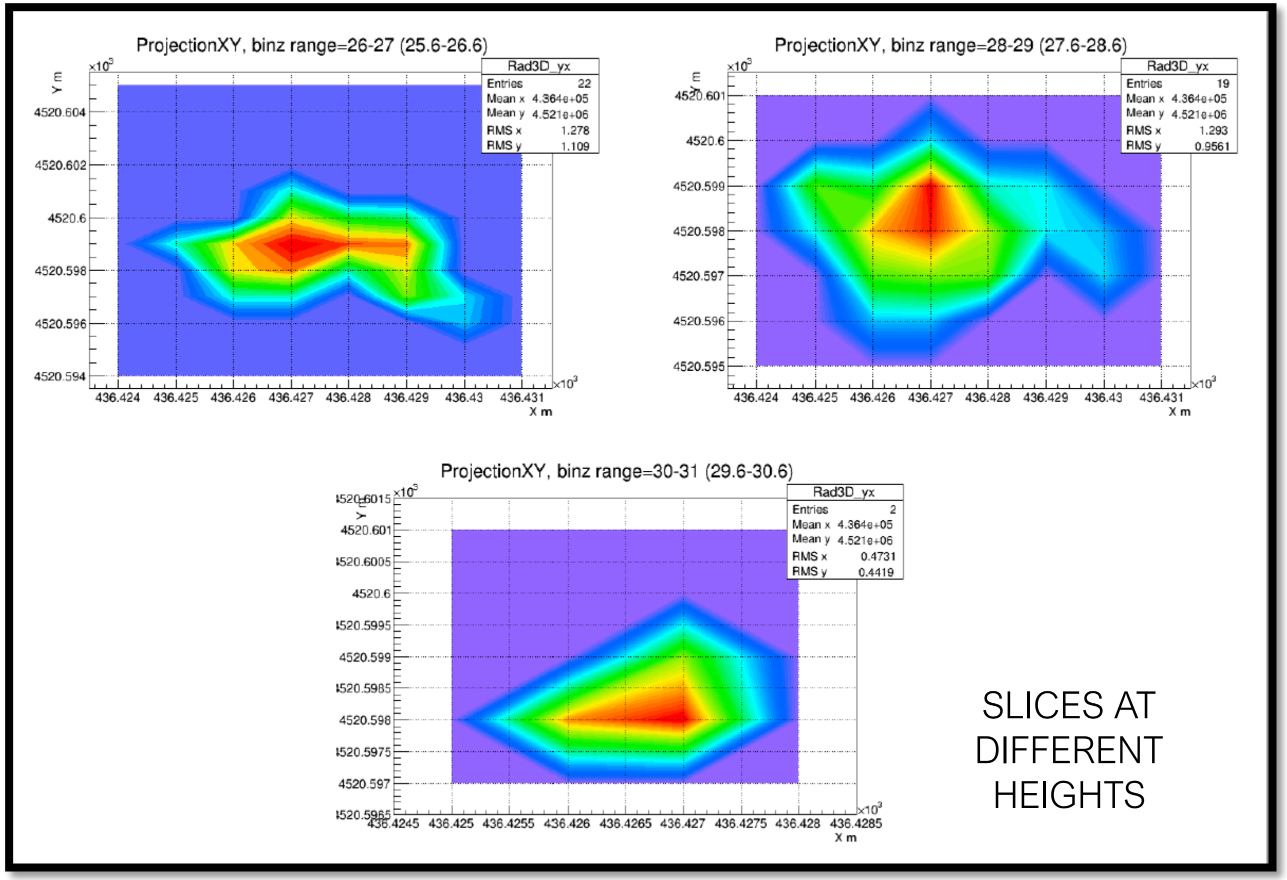


SLICES AT DIFFERENT HEIGHTS

3D RECONSTRUCTED

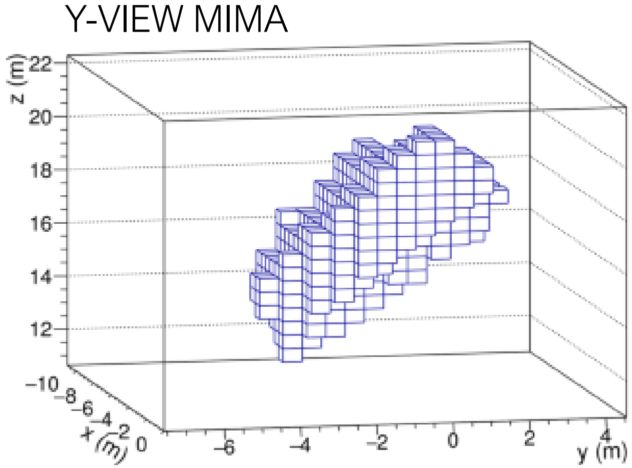


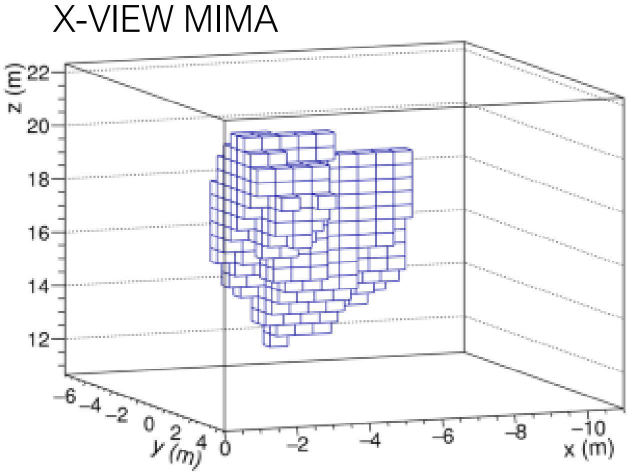

# COMPUTIZED TECHNIQUES

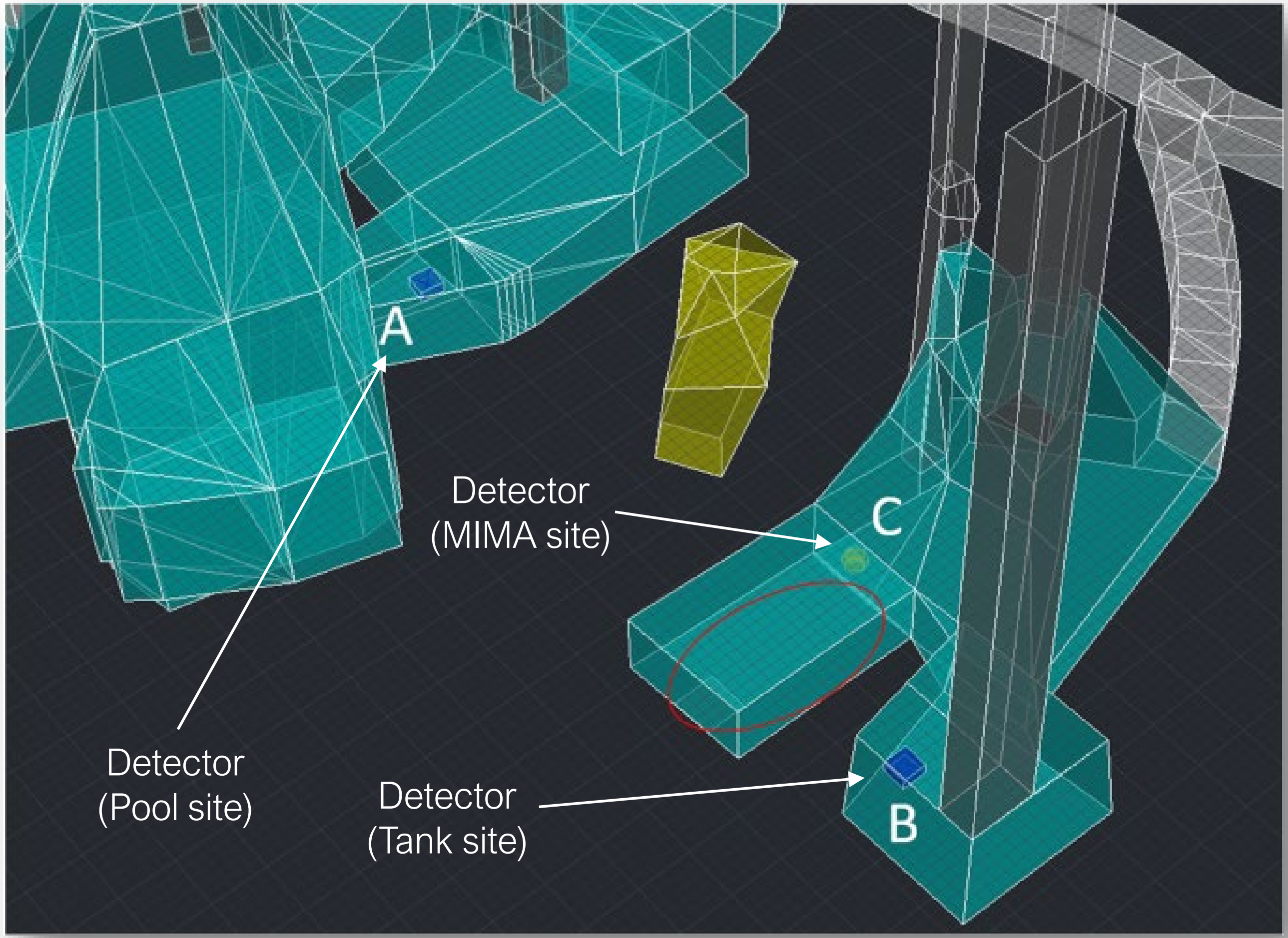


Once modelled the hidden chamber, we made a countercheck by simulating its volume.

Concerning the muographic records, such a cavity implies the existence of two other empty structures…

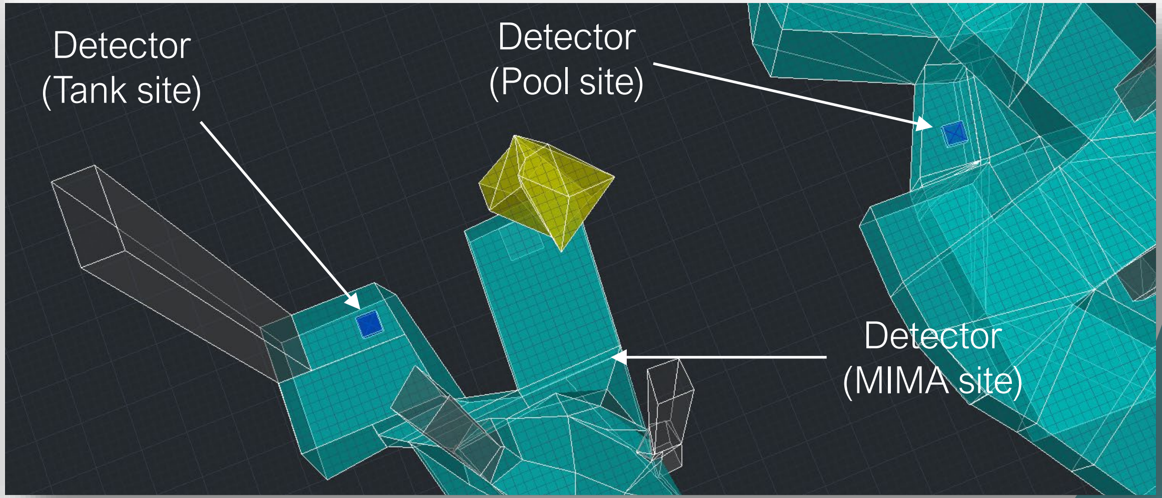

# COMPUTIZED TECHNIQUES

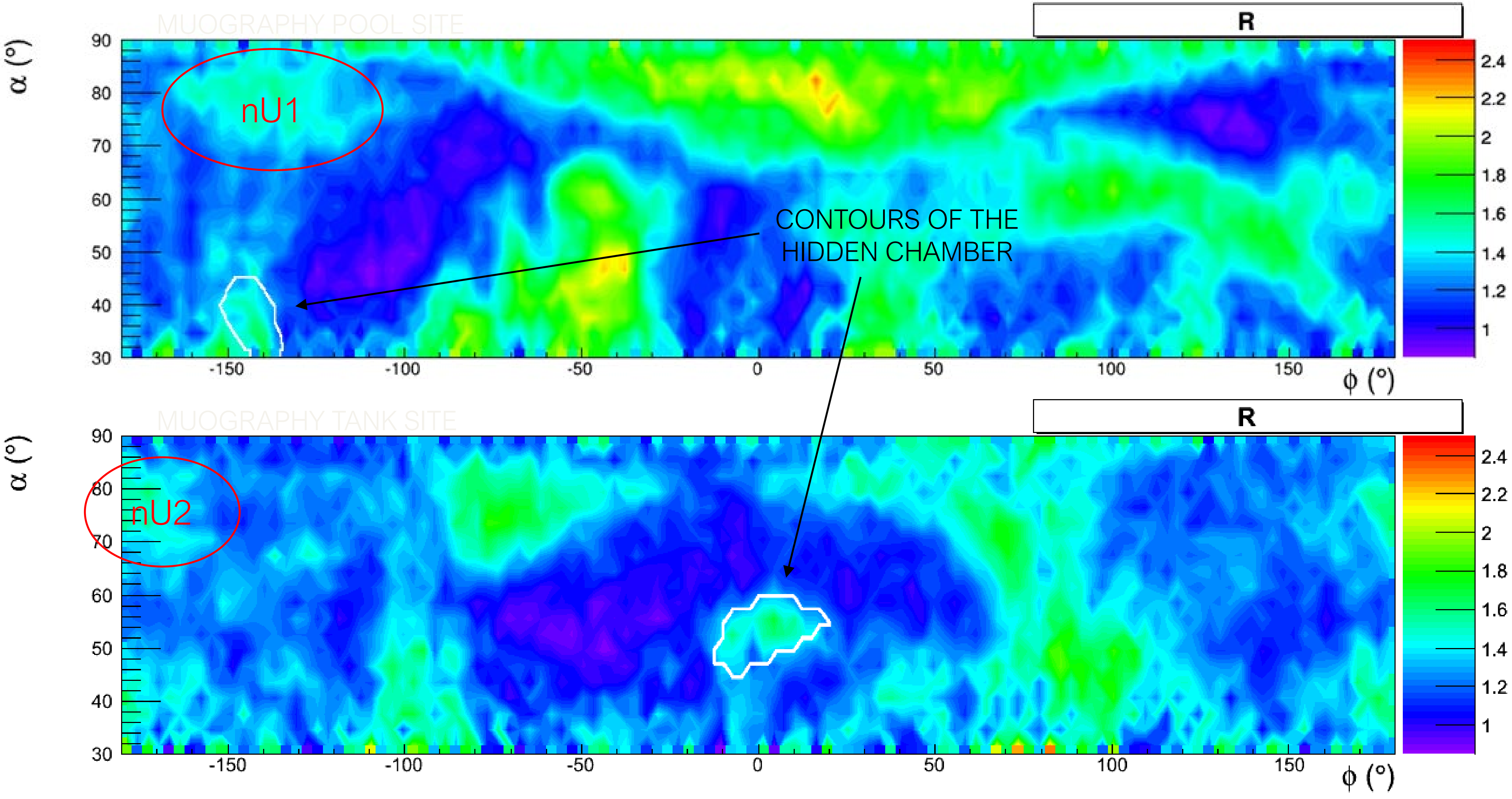

# FUTURE DEVELOPMENTS

# FUTURE DEVELOPMENTS

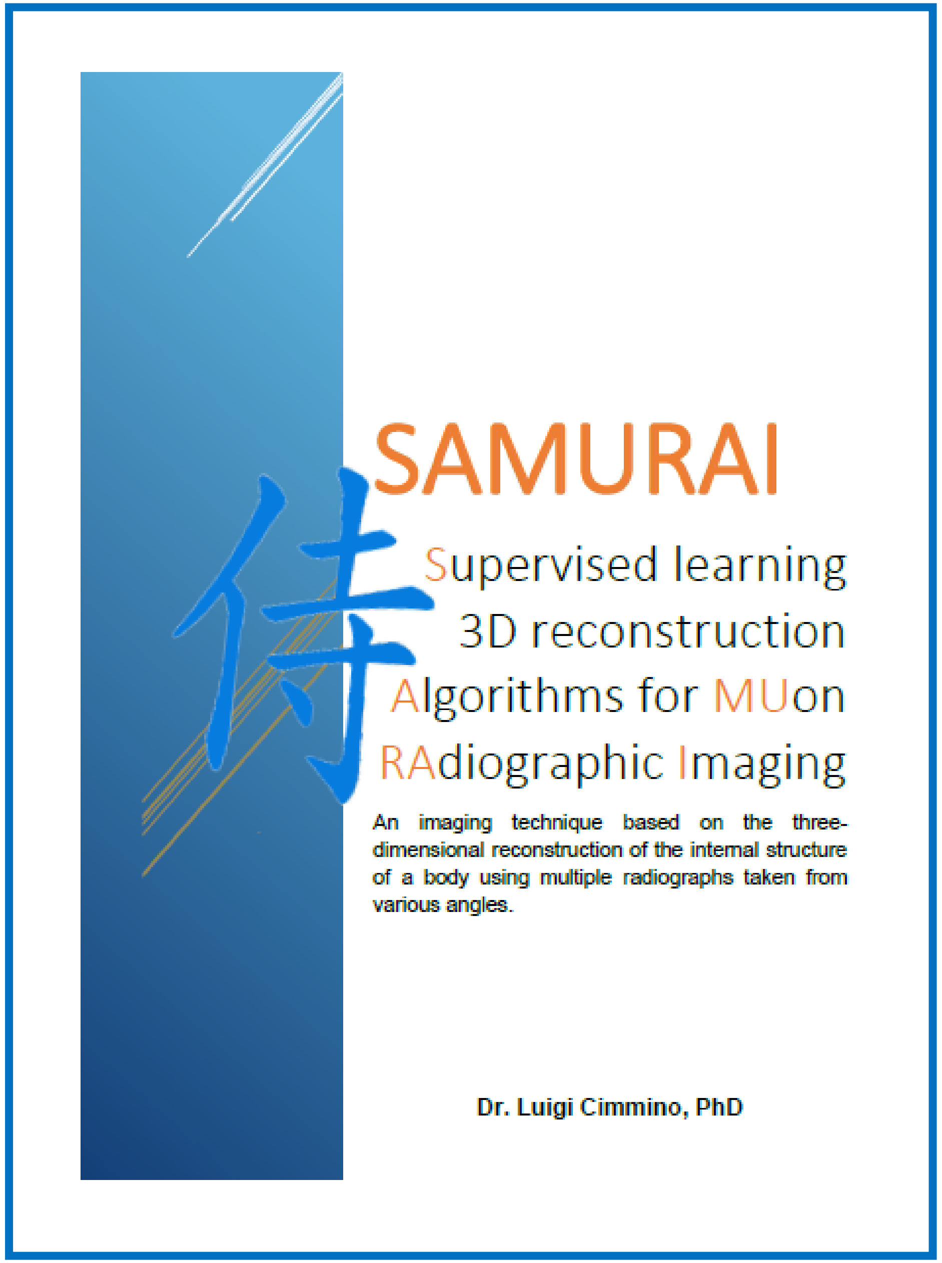


MODE

Machine-learning Optimized Design of Experiments

These are projects that want to apply the latest technological innovation, machine learning, to the three-dimensional reconstruction starting from multiple radiographs and the optimization of detectors to improve their design.